Lawrence Berkeley National Laboratory
Recent Work

Title

TOPICS IN PHENOMENOLOGY OF UNIFIED GAUGE THEORIES OF WEAK, ELECTROMAGNETIC AND STRONG INTERACTIONS

Permalink

https://escholarship.org/uc/item/7cf3z54r

Author

Young, S.K.

Publication Date

1982-11-01

eScholarship.org Powered by the California Digital Library
University of California

LBL-15244

Lawrence Berkeley Laboratory
UNIVERSITY OF CALIFORNIA

Physics, Computer Science & Mathematics Division

RECEIVED
LAWRENCE
BERKELEY LABORATORY
JAN 14 1983
LIBRARY AND
DOCUMENTS SECTION

TOPICS IN PHENOMENOLOGY OF UNIFIED GAUGE THEORIES OF WEAK, ELECTROMAGNETIC, AND STRONG INTERACTIONS

Young Suk Kang
(Ph.D. thesis)

November 1982

Prepared for the U.S. Department of Energy under Contract DE-AC03-76SF00098

LBL-15244

DISCLAIMER

This document was prepared as an account of work sponsored by the United States Government. While this document is believed to contain correct information, neither the United States Government nor any agency thereof, nor the Regents of the University of California, nor any of their employees, makes any warranty, express or implied, or assumes any legal responsibility for the accuracy, completeness, or usefulness of any information, apparatus, product, or process disclosed, or represents that its use would not infringe privately owned rights. Reference herein to any specific commercial product, process, or service by its trade name, trademark, manufacturer, or otherwise, does not necessarily constitute or imply its endorsement, recommendation, or favoring by the United States Government or any agency thereof, or the Regents of the University of California. The views and opinions of authors expressed herein do not necessarily state or reflect those of the United States Government or any agency thereof or the Regents of the University of California.

November 1982 LBL-15244

TOPICS IN PHENOMENOLOGY OF UNIFIED GAUGE THEORIES OF WEAK, ELECTROMAGNETIC, AND STRONG INTERACTIONS*

Young Suk Kang

Ph.D. Thesis

Lawrence Berkeley Laboratory
and
Department of Physics
University of California
Berkeley, California 94720

*This work was supported by the Director, Office of Energy Research, Office of High Energy and Nuclear Physics, Division of High Energy Physics of the U.S. Department of Energy under Contract DE-AC03-76SF

TOPICS IN PHENOMENOLOGY OF UNIFIED GAUGE THEORIES OF WEAK, ELECTROMAGNETIC, AND STRONG INTERACTIONS

by

Young Suk Kang

ABSTRACT

Three phenomenological analyses on the current unification theories of elementary particle interactions are presented. In Chapter I, the neutral current phenomenology of a class of supersymmetric SU(2) X U(1) X $\tilde{U}(1)$ models is analyzed. A model with the simplest fermion and Higgs structure allowing a realistic mass spectrum is considered first. Its neutral current sector is parametrized in terms of two mixing angles and the strength of the new $\tilde{U}(1)$ interactions. Expressions for low-energy model-independent parameters are derived and compared with those of the standard model. Bounds on the neutral gauge boson masses are obtained from the data for various neutrino interactions, eD scattering, and the asymmetry in $e^+e^- \rightarrow \mu^+\mu^-$. A similar analysis is performed on models in which a set of isosinglet Higgs fields contribute to the neutral gauge boson mass matrix. Other predictions of these models which may be relevant to future experiments are discussed.

In Chapter II, the evolution of fermion mass in grand unified theories is reexamined. In particular, the question of gauge invariance of mass ratios in left-right asymmetric theories is

considered. A simple expression is derived for the evolution of the Higgs-fermion-fermion coupling which essentially governs the scale dependence of fermion mass. At the one loop level the expression is gauge invariant and involves only the representation content of left- and right-handed fermions but not that of Higgs. The corresponding expression for supersymmetric theories is also given. Some applications of these formulas are presented.

In Chapter III, the production and the subsequent decays of a heavy lepton pair $L^{\pm}$ near the Z peak in $e^{+}e^{-}$ annihilation are considered as a test of the standard model. The longitudinal polarization is derived from the spin-dependent production cross-section, and the decays $L \to \pi\nu$ and $L \to \ell\nu\nu$ are used as helicity analyzers. The improvement over previous treatments is two-fold: (1) the formulas derived here may be useful for any sequential lepton of mass $\lesssim \frac{M_z}{2}$, and (2) the correlation between the spins of a heavy lepton pair is studied in the form of a cross-section for the production and the coincident decays of the pair.

Dedicated

to

my parents

ACKNOWLEDGEMENTS

My sincere thanks first go to my thesis advisor, Dr. Robert Cahn, without whose guidance this thesis would not have been possible. His willingness to offer help in matters outside physics is also greatly appreciated. I am very grateful to Prof. Mahiko Suzuki for serving as my faculty advisor during my research at Lawrence Berkeley Lab. Dr. Ian Hinchliffe contributed considerably to my thesis research during its later stages. I thank all members of my qualifying exam and thesis committees for their time, especially Prof. Herbert Steiner who helped me much throughout my graduate years. I had the fortune of knowing and working with many friends and colleagues in Berkeley. Among them are Philippe DeForcrand, Chang Gil Han, P.Q. Hung, Jisoon Ihm, and John Northrup. Last but not least, I thank Chisoon for enriching my life.

TABLE OF CONTENTS

I. NEUTRAL CURRENT PHENOMENOLOGY OF SUPERSYMMETRIC $SU(2) \times U(1) \times \tilde{U}(1)$ MODELS

INTRODUCTION

Although the initial development of supersymmetric gauge theories [1] had broad theoretical implications, the recent application of ideas from supersymmetry in particle physics has focused on the hope that an outstanding problem in unified gauge theories of weak, electromagnetic, and strong interactions may be partially solved[2]. While grand unified theories (GUTs) [3] represent a giant step forward in putting all elementary particle interactions on a simpler conceptual basis, part of the price paid in the process is that the problem of the scalar sector is more pronounced than in the standard electroweak model of Glashow, Weinberg, and Salam (GWS) [4]. The scale of SU(2) X U(1) breaking, which is essentially a free parameter in GWS, becomes even more mysterious in GUTs where the natural scale for the theory appears to be that of the breaking of the grand unifying group, M_x (perhaps identifiable with the Planck mass, M_p). In addition, the quadratic divergences that plague elementary scalars in GWS still remain to make GUTs unnatural. The so-called gauge-hierarchy problem consists of: (I) why at the tree level there exist two vastly different scales, and (II) why radiative corrections do not generate a new scale, say, of the order of αM_x, which means in every order in perturbation theory there should be miraculous cancellations which preserve the tree level symmetry breaking pattern.

Supersymmetry can provide a partial answer to this problem by putting scalars in the same supermultiplet as fermions, thus

preventing some scalars from getting large masses, as their fermionic partners are protected by chiral symmetry. Non-renormalization properties of supersymmetric theories [5] further ensure that these scalar fields do not develop quadratic divergences. This has been the main motivation behind recent "low energy" supersymmetric models [2] in which supersymmetry persists down to the GWS breaking scale. In fact, it turns out that in many models scalars that remain almost massless are not easily generated, and to date there exists no realistic GUT which incorporates supersymmetry. It was shown explicitly, however, that at least in some toy models [6] the existence of such scalars is indeed possible, and one may continue to be optimistic about the role supersymmetry might play in unified theories.

Among a number of constraints supersymmetric theories face, perhaps the most obvious one is that supersymmetry should be broken at low energy since scalar partners of quarks and leptons have not been observed yet experimentally. The breaking can be either explicit or spontaneous. In the case of explicit supersymmetry breaking, scalar partners of ordinary fermions can obtain arbitrarily large masses, as mass terms are added directly to the Lagrangian, provided they remain soft, i.e., they do not introduce quadratic divergences [7]. On the other hand, spontaneous supersymmetry breaking at the tree level requires that a certain relation be satisfied among masses of particles with different spins, as explained in detail in Section 1. Because of this constraint, supersymmetric theories based on the standard internal symmetry group SU(3) X SU(2) X U(1) do not have a realistic mass spectrum. It is in this context that Fayet [8] proposed the

extension of the standard gauge group to include an extra $\tilde{U}(1)$ factor under which known fermions transform chirally. This type of extra gauge symmetry was also considered to be a possible mechanism for preventing nucleons from decaying too fast [9].

The introduction of such a new gauge interaction brings about new theoretical and phenomenological complications. On the theoretical front, it was shown that a consistent model can be constructed which is anomaly-free and which has the correct vacuum structure [2]. Some of the new phenomenology due to a new neutral gauge boson associated with $\tilde{U}(1)$ has been considered by Fayet [10]. It is the purpose of this chapter to parametrize and analyze systematically the neutral current sector of a rather general class of supersymmetric "extra $\tilde{U}(1)$" models.

It turns out that this analysis often parallels what was done on a number of alternative electroweak models of the past with more than one neutral boson, most notable of which include $SU(2)_L \times SU(2)_R \times U(1)$ [11] and $SU(2)_L \times U(1) \times U(1)$ [12]. Some of these models typically were motivated to accommodate apparent deviations of some experimental data from the standard model predictions at the time. Others were introduced mainly for the sake of considering alternatives to orthodoxy. Although some models had theoretical implications, for example as a possible effective group surviving at low energy when a certain grand unifying group breaks [13], the class of supersymmetric extra $\tilde{U}(1)$ models considered here enjoy a more compelling theoretical motivation than most other alternative models.

The organization of this chapter is as follows. In Section 1, the essential features of supersymmetric extra $\tilde{U}(1)$ models are reviewed. The theoretical motivation, the structure of Higgs and fermion sectors, and the neutral vector boson mass matrix are discussed. In Section 2, the minimal mixing model, defined at the end of Section 1, is analyzed. After the parametrization of the model is given, expressions for low energy model independent parameters are derived in terms of the model parameters. A fit is made to the low energy data from neutrino scattering [14] and SLAC eD experiments [15]. The forward-backward asymmetry in $e^+e^- \to \mu^+\mu^-$ is derived, and along with the fit made previously, bounds on the vector boson masses are estimated from the recent DESY [17-20] data for the asymmetry. In Section 3, an extension of the minimal mixing model is made to include contributions from isosinglet Higgs fields. This section parallels Section 2; model independent parameters are derived and fits to data are obtained. In Section 4, other neutral current processes which can be potentially affected by the extra $\tilde{U}(1)$ are considered. The decay widths of the neutral bosons, and the anomalous magnetic moment of the muon are discussed. Section 5 contains a summary and conclusions.

1. SUPERSYMMETRIC SU(2) X U(1) X $\tilde{U}(1)$ MODELS

(i) Motivation for the Extra U(1) and the Structure of the Fermion Sector

If supersymmetry is relevant in particle physics, it must be broken at low energy since Bose-Fermi mass degeneracy is not observed in nature. If the breaking is spontaneous, there exists at the tree level the following mass relation for particles with different

spins [21];

$$\sum_J (-1)^{2J}(2J+1)\ \mathrm{tr}\ M_J^2 = \sum_\alpha C_\alpha\ \mathrm{tr}\ q^\alpha, \qquad (1)$$

where M_J is the mass matrix for a spin J field, and q^α the charge of a chiral multiplet for a gauge group labeled by α. C_α is a constant which depends on the group and the supersymmetry breaking parameter.

If we use the standard gauge group, and enlarge each weak multiplet to include supersymmetric partners, eq. (1) results in an unacceptable mass relation [22]. For SU(3) X SU(2) X U(1) the right-hand side of eq. (1) is zero, and for a four-component fermion f, we get

$$M_s^2 + M_t^2 = 2\ M_f^2\ , \qquad (2)$$

where s and t are the two scalar partners corresponding to, say, the left-handed and the right-handed components of f. No scalar particles satisfying eq. (2) have been seen for any of the three generations of four-component fermions with the possible exception of the yet undiscovered top quark.

One solution to this problem was suggested by Fayet [10], who introduced a new gauge group $\tilde{U}(1)$ which couples chirally to fermions. We then have the relations

$$M_s^2 - M_f^2 = (\mathrm{const})\ \tilde{Q}_L$$

$$M_t^2 - M_f^2 = -\ (\mathrm{const})\ \tilde{Q}_R\ , \qquad (3)$$

where $\tilde{Q}_L$ and $\tilde{Q}_R$ are the $\tilde{U}(1)$ charges of left- and right-handed f. It is obvious from eq. (3) that for both s and t to be heavier than f, $\tilde{Q}_L$ and $\tilde{Q}_R$ should have opposite signs. In other words, the minimum requirement for the $\tilde{U}(1)$ charge of a four-component Dirac fermion is that its axial part should be larger in magnitude than its vector part. There is no such restriction on neutrino $\tilde{U}(1)$ couplings in theories where right-handed neutrinos are absent.

In the most general supersymmetric extra $\tilde{U}(1)$ model satisfying this requirement, different fermions can in principle couple to $\tilde{U}(1)$ differently, which will result in the proliferation of parameters in the fermion sector. However, there are arguments suggesting that masses of some scalars are almost degenerate. For example, the scalar partners of u and d quarks, pairwise, based on measurements of parity violating nuclear transitions, appear to have small mass differences, unless the masses are greater than 0(100) GeV [23]. Also, the limits on flavor changing neutral currents suggest that the scalar partners of quarks and leptons with the same quantum numbers but in different generations are nearly degenerate in mass [24]. Thus the $\tilde{U}(1)$ couplings of at least some fermions seem to have the same axial part and negligible vector parts.

In view of these considerations we use throughout this chapter the simplest fermionic $\tilde{U}(1)$ couplings meeting the mass requirement. A straightforward supersymmetric generalization of the standard model particle assignment is made; left-handed matter supermultiplets consist of

$$Q_L = \begin{pmatrix} U_L \\ D_L \end{pmatrix}, \quad \bar{U}_R, \quad \bar{D}_R, \quad L_L = \begin{pmatrix} N_L \\ E_L \end{pmatrix}, \quad \bar{E}_R,$$

whose fermionic components are the ordinary quarks and leptons. These fields have the usual SU(3) X SU(2) X U(1) quantum numbers while all of them have the same $\tilde{U}(1)$ charge, $\frac{\tilde{y}}{2}$. This means that quarks and charged leptons have the identical, purely axial $\tilde{U}(1)$ charge, $\tilde{y}$, and the neutrino has a V-A coupling, $\frac{\tilde{y}}{2}$, to $\tilde{U}(1)$. The quantum numbers of these fields are listed in Table 1. Any extension of this minimal structure finds little theoretical motivation in actual models, and will not be considered here. We note in passing that Fayet [10], in comparing the predictions of supersymmetric extra $\tilde{U}(1)$ models with neutrino data, introduced the parameters cos ϕ_u, cos ϕ_d, etc., corresponding to the magnitude of the vector parts of the $\tilde{U}(1)$ couplings for u, d, etc., relative to their axial parts.

(ii) The Higgs Structure

Unlike in the standard model where a single Higgs isodoublet gives mass to both charge $\frac{2}{3}$ and $-\frac{1}{3}$ quarks, in supersymmetric models at least two isodoublets, ϕ_1, and ϕ_2, are required, since superfields within the same term in the Lagrangian should be of the same chirality. From the Yukawa terms $\bar{Q}_L \phi_1 U_R$ and $\bar{Q}_L \phi_2 D_R$, we see that the U(1) charges of ϕ_1 and ϕ_2 differ by one and their $\tilde{U}(1)$ charges are the same. These Higgs fields, as in the standard model, also serve to break SU(2) X U(1).

Other Higgs fields may be needed, for example, for theoretical consistency such as the correct vacuum structure [2,25]. Some of them may alter the neutral current sector as they obtain non-zero vacuum expectation values (VEV's). One such set of Higgs fields occurring in actual models will be considered in Section 3, namely, those which transform trivially under SU(2) X U(1) and non-trivially under $\tilde{U}(1)$.

(iii) The Neutral Boson Mass Matrix

The covariant derivatives for the two Higgs isodoublets described above are:

$$D_\mu\phi_1 = (\partial_\mu - ig_2 \frac{\vec{\tau}}{2} \cdot \vec{W}_\mu - iy_1 g B_\mu - i\,\tilde{y}\,\tilde{g}\,\tilde{B}_\mu)\,\phi_1 \qquad (4a)$$

$$D_\mu\phi_2 = (\partial_\mu - ig_2 \frac{\vec{\tau}}{2} \cdot \vec{W}_\mu - iy_2 g B_\mu - i\,\tilde{y}\,\tilde{g}\,\tilde{B}_\mu)\,\phi_2\ , \qquad (4b)$$

where $\vec{W}_\mu$, B_μ, $\tilde{B}_\mu$ are the boson fields, and g_2, g, $\tilde{g}$ the couplings associated with SU(2), U(1), $\tilde{U}(1)$, respectively. y_1 and y_2, the U(1) charges of ϕ_1, and ϕ_2, satisfy $y_1 = y_2 + 1$ from the Yukawa terms, and $\tilde{y}$ is the common $\tilde{U}(1)$ charge of ϕ_1 and ϕ_2, which is twice that of left-handed fermions.

As ϕ_1 and ϕ_2 obtain VEV's,

$$\phi_1 = \begin{pmatrix} 0 \\ h_1 \end{pmatrix} \qquad \phi_2 = \begin{pmatrix} h_2 \\ 0 \end{pmatrix}, \qquad (5)$$

the terms relevant to masses in the Lagrangian become:

$$(D_\mu\phi_1)^\dagger(D^\mu\phi_1) \sim h_1^2\,\{(\frac{g_2}{2} W_\mu^3 - y_1 g B_\mu - \tilde{y}\,\tilde{g}\,\tilde{B}_\mu)^2 + \frac{g_2^2}{4}(W_\mu^\pm)^2\} \qquad (6a)$$

$$(D_\mu \phi_2)^\dagger (D^\mu \phi_2) \sim h_2^2 \{ (\frac{g_2}{2} W_\mu^3 + y_2 g B_\mu + \tilde{y}\tilde{g}\tilde{B}_\mu)^2 + \frac{g_2^2}{4} (W_\mu^\pm)^2 \} \tag{6b}$$

The mass of the charged weak bosons is given by

$$M_{W^\pm}^2 = \frac{g_2^2}{4}(h_1^2 + h_2^2) \ . \tag{7}$$

The neutral boson mass matrix becomes:

$$M^2 = \begin{array}{c} \\ \\ \\ \end{array} \begin{array}{c} \begin{array}{ccc} B_\mu & W_\mu^3 & \tilde{B}_\mu \end{array} \\ \begin{bmatrix} g^2(y_1^2 h_1^2 + y_2^2 h_2^2) & \frac{g g_2}{2}(y_2 h_2^2 - y_1 h_1^2) & g\tilde{y}\tilde{g}(y_1 h_1^2 + y_2 h_2^2) \\ \frac{g g_2}{2}(y_2 h_2^2 - y_1 h_1^2) & \frac{g_2}{4}(h_1^2 + h_2^2) & \frac{g_2}{2}\tilde{y}\tilde{g}(h_2^2 - h_1^2) \\ g\tilde{y}\tilde{g}(y_1 h_1^2 + y_2 h_2^2) & \frac{g_2}{2}\tilde{y}\tilde{g}(h_2^2 - h_1^2) & \tilde{y}^2\tilde{g}^2(h_1^2 + h_1^2) \end{bmatrix} \end{array} \tag{8}$$

Notice that $\det M^2 = 0$ regardless of y_1, y_2, h_1, h_2, since the VEV's of ϕ_1 and ϕ_2 have been chosen such that electromagnetism is unbroken.

The eigenvector of the mass matrix (8) corresponding to the photon is given by

$$A_\mu = \frac{\tilde{y}\tilde{g} g_2 B_\mu + \tilde{y}\tilde{g}(y_1 - y_2) g W_\mu^3 - g_2 g \frac{y_1 + y_2}{2} \tilde{B}_\mu}{\left[\tilde{y}^2\tilde{g}^2 g_2^2 + (y_1 - y_2)^2 g^2 \tilde{y}^2 \tilde{g}^2 + g_2^2 g^2 (\frac{y_1 + y_2}{2})^2\right]^{1/2}} \ . \tag{9}$$

If $y_1 = -y_2$, A_μ has no contribution from $\tilde{B}_\mu$, and the mixing for A_μ is as in the standard model; $Q=T_3+Y$, where Y is the $U(1)$ generator and $A_\mu = \cos\theta B_\mu + \sin\theta W^3_\mu$, where $\sin^2\theta = \frac{g^2}{g^2+g_2^2}$ is the usual weak mixing parameter. The quantum numbers of ϕ_1 and ϕ_2 are shown in Table 1. Of course one can be completely general and consider full mixing of all three neutral boson fields involving three different mixing angles. However, our aim in this chapter is to analyze the most economical class of models theoretical consistency allows. Thus we leave the photon the same as in the standard model, while we introduce mixing between the two massive neutral bosons in order to avoid immediate contradiction with data, as discussed in Section 2.

With $y_1 = -y_2 = \frac{1}{2}$, the mass matrix (8) now becomes

$$M^2 = \frac{1}{4}(h_1^2+h_2^2)\begin{bmatrix} g^2 & -gg_2 & -g\bar{g}\epsilon \\ -gg_2 & g_2^2 & g_2\bar{g}\epsilon \\ -g\bar{g}\epsilon & g_2\bar{g}\epsilon & \bar{g}^2 \end{bmatrix}, \qquad (10)$$

where $\epsilon = \frac{h_1^2-h_2^2}{h_1^2+h_2^2}$, and $\bar{g} = -2\tilde{y}\tilde{g}$.

ϵ is a measure of the mixing between the two massive neutral bosons. If $h_1^2=h_2^2$ ($\epsilon=0$), $\tilde{B}_\mu$ decouples completely from B_μ and W^3_μ, and $\tilde{g}$ alone sets the scale of the $\tilde{U}(1)$ breaking. The minimal mixing model (MMM) is now defined as the one in which there are two Higgs isodoublets whose neutral components obtain different VEV's in general.

2. THE MINIMAL MIXING MODEL

(i) Parametrization

Here we parametrize the neutral current sector of MMM defined at the end of Section 1, and list formulas useful in deriving expressions for the low-energy model-independent neutral current parameters.

The mass matrix and one of the eigenvectors A_μ were written down in Section 1. The other two eigenvectors Z_μ, $\tilde{Z}_\mu$ with non-zero eigenvalues M_z^2, $M_{\tilde{z}}^2$ are:

$$Z_\mu = \frac{1}{\sqrt{g^2 + g_2^2 + \bar{g}^2\eta^2}} \left(-gB_\mu + g_2 W_\mu^3 + \bar{g}\eta\tilde{B}_\mu\right) \tag{1a}$$

$$\tilde{Z}_\mu = \frac{1}{\sqrt{g^2\tilde{\eta}^2 + g_2^2\tilde{\eta}^2 + \bar{g}^2}} \left(-g\tilde{\eta}B_\mu + g_2\tilde{\eta}W_\mu^3 + \bar{g}\tilde{B}_\mu\right) , \tag{1b}$$

where

$$\eta = \frac{\varepsilon}{1 - \bar{g}^2\,(1-\varepsilon^2)\,\dfrac{\frac{1}{4}\,(h_1^2 + h_2^2)}{M_z^2}} , \tag{2a}$$

$$\tilde{\eta} = \frac{\varepsilon}{1 - (g^2 + g_2^2)\,(1-\varepsilon^2)\,\dfrac{\frac{1}{4}\,(h_1^2 + h_2^2)}{M_z^2}} . \tag{2b}$$

The expressions (1) have been chosen so that as ε tends to zero the detachment of $\tilde{U}(1)$ from SU(2) X U(1) is smoothly made. (In this limit $\eta, \tilde{\eta} \to 0$.) Note that $\eta\tilde{\eta} = 1$ if $M_z = M_{\tilde{z}}^2$.

We now write the eigenvectors as follows:

$$\begin{bmatrix} A_\mu \\ Z_\mu \\ \tilde{Z}_\mu \end{bmatrix} = \begin{bmatrix} \cos\theta & \sin\theta & 0 \\ -\cos\alpha\sin\theta & \cos\alpha\cos\theta & \sin\alpha \\ \sin\alpha\sin\theta & -\sin\alpha\cos\theta & \cos\alpha \end{bmatrix} \begin{bmatrix} B_\mu \\ W^3_\mu \\ \tilde{B}_\mu \end{bmatrix} , \tag{3}$$

where θ was defined in Section 1, and

$$\cos^2\alpha = \frac{g^2 + g_2^2}{g^2 + g_2^2 + \bar{g}^2\eta^2} \tag{4}$$

The sign of $\cos\alpha$ is chosen to be positive, and the sign of $\sin\alpha$ will be discussed later in terms of other parameters. As mentioned before, of the three rotation angles one was eliminated by requiring that the photon does not mix with the $\tilde{U}(1)$ boson.

The non-zero eigenvalues of the mass matrix satisfy the following:

$$\rho + \tilde{\rho} = 1 + A$$
$$\rho\tilde{\rho} = A(1-\varepsilon^2) , \tag{5}$$

$$\text{where } \rho = \frac{M_z^2\cos^2\theta}{M_W^2} , \quad \tilde{\rho} = \frac{M_{\tilde{z}}^2\cos^2\theta}{M_W^2} , \tag{6}$$

i.e., mass squared in units of the standard model Z mass squared, and

$$A \equiv \frac{\bar{g}^2}{g^2 + g_2^2} = \frac{\bar{g}^2\cos^2\theta\sin^2\theta}{e^2} . \tag{7}$$

Requiring that as $\varepsilon \to 0$, $\rho \to 1$ and $\tilde{\rho} \to A$, we identify

$$\rho = \frac{1}{2}\left[1 + A + (1 - A)\sqrt{1 + \frac{4A\varepsilon^2}{(1 - A)^2}}\,\right] \tag{8a}$$

$$\tilde{\rho} = \frac{1}{2}\left[1 + A - (1 - A)\sqrt{1 + \frac{4A\varepsilon^2}{(1 - A)^2}}\,\right] . \tag{8b}$$

Which boson mass is the bigger depends on whether A is larger than unity or not:

$$(A - 1)\ (\tilde{\rho} - \rho) \geq 0 .$$

Also notice that $(1 - \rho)\ (1 - \tilde{\rho}) = -A\varepsilon^2 \leq 0$, which means one boson is lighter and the other is heavier than the standard model Z mass. Thus the Georgi-Weinberg theorem [26] on neutral boson masses in a multi-boson model is satisfied, although its premise is not met.

It turns out that ρ and $\tilde{\rho}$ are very convenient intermediate parameters to work with. For example, in terms of ρ and $\tilde{\rho}$,

$$\eta = \frac{\varepsilon}{1 - \tilde{\rho}} \quad , \qquad \tilde{\eta}^{-1} = \frac{\varepsilon}{1 - \rho} \quad , \tag{9a,b}$$

which give

$$\cos\alpha = \sqrt{\frac{1 - \tilde{\rho}}{\rho - \tilde{\rho}}} \quad , \qquad \sin\alpha = \pm \sqrt{\frac{\rho - 1}{\rho - \tilde{\rho}}} \quad . \tag{10a,b}$$

The sign of $\sin\alpha$ is such that if $(1 - A)\varepsilon \geq 0$, $\sin\alpha \geq 0$, and vice versa. From eqs. (8) and (10),

$$\cos\alpha = \left\{\frac{1}{2}\left(1 + \left[1 + \frac{4A\,\varepsilon^2}{(1 - A)^2}\right]^{-\frac{1}{2}}\right)\right\}^{\frac{1}{2}} . \tag{11}$$

There are five independent parameters in MMM: $g, g_2, \tilde{g}, h_1, h_2$. Apart from

$$e = \frac{g g_2}{\sqrt{g^2 + g_2^2}} \quad , \quad G_F = \frac{\sqrt{2}\, g_2^2}{8 M_W^2} = \frac{1}{\sqrt{2}\,(h_1^2 + h_2^2)} \quad , \tag{12a,b}$$

we choose to work with the following three free parameters: $\sin^2\theta$, as in the standard model, and $A \geq 0$, $|\,\varepsilon\,| \leq 1$, which measure the relative strength of the $\tilde{U}(1)$ coupling, and the degree of mixing between the two massive neutral bosons, respectively. We will eventually express low energy model independent parameters in terms of these model parameters.

We now consider the couplings of fermion f to Z_μ and $\tilde{Z}_\mu$. In terms of physical fields the relevant interaction terms in the Lagrangian are written as follows:

$$\mathscr{L}_{int} = A^\mu \sum_f (Q^\gamma J_\mu^V)_f + Z^\mu \sum_f (Q_Z^V J_\mu^V + Q_Z^A J_\mu^A)_f + \tilde{Z}^\mu \sum_f (Q_{\tilde{Z}}^V J_\mu^V + Q_{\tilde{Z}}^A J_\mu^A)_f \,, \tag{13}$$

where $J_\mu^V = \bar{f}\gamma_\mu f$, $J_\mu^A = \bar{f}\gamma_\mu\gamma_5 f$. Q^γ is the electric charge, and Q_Z^V, $Q_{\tilde{Z}}^V$ are vector, and Q_Z^A, $Q_{\tilde{Z}}^A$ axial weak charges.

The weak charges are given by:

$$Q_Z^V = \frac{e}{\sin\theta\cos\theta}\cos\alpha\left[\frac{T_{3R} + T_{3L}}{2} - Q^\gamma \sin^2\theta\right] + \tilde{g}\sin\alpha\,\frac{\tilde{Y}_L + \tilde{Y}_R}{2} \tag{14a}$$

$$Q_Z^A = \frac{e}{\sin\theta\cos\theta}\cos\alpha\,\frac{T_{3R}-T_{3L}}{2} + \tilde{g}\,\sin\alpha\,\frac{\tilde{Y}_R-\tilde{Y}_L}{2} \tag{14b}$$

$$Q_{\tilde{Z}}^V = -\frac{e}{\sin\theta\cos\theta}\sin\alpha\left[\frac{T_{3R}+T_{3L}}{2} - Q^Y\sin^2\theta\right] + \tilde{g}\cos\alpha\,\frac{\tilde{Y}_L+\tilde{Y}_R}{2} \tag{14c}$$

$$Q_{\tilde{Z}}^A = -\frac{e}{\sin\theta\cos\theta}\sin\alpha\,\frac{T_{3R}-T_{3L}}{2} + \tilde{g}\cos\alpha\,\frac{\tilde{Y}_R-\tilde{Y}_L}{2}\ . \tag{14d}$$

For quarks and charged leptons, as discussed in Section 1, we take $\tilde{Y}_L = -\tilde{Y}_R = \frac{\tilde{Y}}{2}$. For neutrinos $\tilde{Y}_R=0$, $\tilde{Y}_L = \frac{\tilde{Y}}{2}$. Thus these charges become, for example, for the electron,

$$Q_{Z,e}^V = -\frac{1}{4}\cos\alpha\,\frac{e}{\sin\theta\cos\theta}\,(1-4\sin^2\theta) \tag{15a}$$

$$Q_{Z,e}^A = \frac{1}{4}\left(\cos\alpha\,\frac{e}{\sin\theta\cos\theta} + \bar{g}\sin\alpha\right) \tag{15b}$$

$$Q_{Z,e}^Y = \frac{1}{4}\sin\alpha\,\frac{e}{\sin\theta\cos\theta}(1 - 4\sin^2\theta) \tag{15c}$$

$$Q_{\tilde{Z},e}^A = \frac{1}{4}\left(-\sin\alpha\,\frac{e}{\sin\theta\cos\theta} + \bar{g}\cos\alpha\right)\ . \tag{15d}$$

For $\alpha=0$ ($\varepsilon=0$, or $\rho=1$) the vector charges are the same as in the standard model and the axial charges contain contributions from $\tilde{U}(1)$.

(ii) Model Independent Parameters

In comparing neutral current predictions of an electroweak model with data it is customary to work with low-energy model independent parameters [27]. Here we derive the expressions for the parameters which describe various low-energy processes involving

space-like momentum transfer, in terms of the MMM parameters, $\sin^2\theta$, A, ε. The model independent parameters we use are defined in the following processes.

1) Neutrino-electron scattering

$$\mathcal{L}_{eff} = -\frac{G}{\sqrt{2}}\bar{\nu}\gamma^{\alpha}(1-\gamma_5)\nu\bar{e}\gamma_{\alpha}(g_V^e + g_A^e\gamma_5)e \qquad (16)$$

The values for g_V^e and g_A^e determined experimentally from ν-e elastic scattering data are given in Table 2.

2) Neutrino-hadron reactions

$$\mathcal{L}_{eff} = -\frac{G}{\sqrt{2}}\bar{\nu}\gamma^{\alpha}(1-\gamma_5)\nu\bar{q}\gamma_{\alpha}(g_V^q + g_A^q\gamma_5)q \quad , \qquad (17)$$

where $q = u$ or d .

The available data for these parameters are from deep inelastic scattering, semi-inclusive pion production, elastic ν p scattering, and other processes [28]. The following linear combinations [27] somewhat facilitate fits to data, as some of them (β and δ) turn out to be independent of $\sin^2\theta$:

$$\alpha = g_V^u - g_V^d \quad \text{(vector isovector)} \qquad (18a)$$

$$\beta = g_A^u - g_A^d \quad \text{(axial isovector)} \qquad (18b)$$

$$\gamma = g_V^u + g_V^d \quad \text{(vector isoscalar)} \qquad (18c)$$

$$\delta = g_A^u + g_A^d \quad \text{(axial isoscalar)} \quad . \qquad (18d)$$

3) ELECTRON-HADRON REACTIONS

$$\mathscr{L}_{eff} = -\frac{G}{\sqrt{2}}\Big\{\bar{e}\gamma^{\alpha}\gamma_5 e\ [C_{1u}\bar{u}\gamma_{\alpha}u + C_{1d}\bar{d}\gamma_{\alpha}d]$$

$$+\ \bar{e}\gamma^{\alpha}e\ [C_{2u}\bar{u}\gamma_{\alpha}\gamma_5 u + C_{2d}\bar{d}\gamma_{\alpha}\gamma_5 d]\Big\} \qquad (19)$$

The parameters C_{1u}, C_{1d}, C_{2u}, C_{2d} describe parity-violating electron-nucleon interactions. Not all of these four parameters have been determined experimentally in a model independent way yet, and the following two combinations are used here:

$$a = -\frac{4}{3}\left(C_{1u} - \frac{1}{2}C_{1d}\right) \qquad (20a)$$

$$b = -\frac{4}{3}\left(C_{2u} - \frac{1}{2}C_{2d}\right) \ . \qquad (20b)$$

a and b enter into the expression for the asymmetry (A_{eD}) in eD scattering [29]:

$$\frac{A_{eD}(y)}{Q^2} = -\frac{9}{20}\frac{G}{\sqrt{2}\pi\alpha_{EM}}\left[a + \frac{1-(1-y)^2}{1+(1-y)^2}\,b\right] \ . \qquad (21)$$

Since it turns out that the error in experimental determination of b is large and the errors for a and b are highly correlated, the following combination which is best determined will be used in place of b [27]:

$$c = a + .25b = -\frac{4}{3}\left(C_{1u} - \frac{1}{2}C_{1d}\right) - \frac{1}{3}\left(C_{2u} - \frac{1}{2}C_{2d}\right) \ . \qquad (22)$$

Various atomic parity violation experiments can also be described by linear combinations of C_{1u}, C_{1d}, C_{2u}, C_{2d}, and analyses of some alternative models have included the recent data [11]. However, in this analysis atomic experiments will not be considered, and a total of eight parameters are studied:

$$g_V^e,\ g_A^e,\ \alpha,\ \beta,\ \gamma,\ \delta,\ a,\ c \quad .$$

We now derive the expressions for these parameters. From eqs. (14), (16), and (17),

$$g_V^f = \frac{M_W^2}{\cos^2\theta} \left\{ \frac{1}{M_Z^2} (\cos\alpha - \frac{1}{2}\frac{\bar{g}}{e} \sin\alpha \sin\theta \cos\theta)[\cos\alpha\ (T_{3L} - 2Q^\gamma \sin^2\theta)] \right.$$
$$\left. + \frac{1}{M_{\tilde{Z}}^2} (\sin\alpha + \frac{1}{2}\frac{\bar{g}}{e} \sin\alpha \sin\theta \cos\theta)[\sin\alpha\ (T_{3L} - 2Q^\gamma \sin^2\theta)] \right\}, \tag{23a}$$

$$g_A^f = \frac{M_W^2}{\cos^2\theta} \left\{ \frac{1}{M_Z^2} (\cos\alpha - \frac{1}{2}\frac{\bar{g}}{e} \sin\alpha \sin\theta \cos\theta)[-\cos\alpha\ T_{3L} \right.$$
$$+ \frac{1}{2}\frac{\bar{g}}{e} \sin\alpha \sin\theta \cos\theta] - \frac{1}{M_{\tilde{Z}}^2} (\sin\alpha + \frac{1}{2}\frac{\bar{g}}{e} \cos\alpha \sin\theta \cos\theta)$$
$$\left. [\sin\alpha\ T_{3L} + \frac{1}{2}\frac{\bar{g}}{e} \cos\alpha \sin\theta \cos\theta] \right\}, \tag{23b}$$

where f = e, u, or d.

Eqs. (23) are written again as:

$$g_V^f = (T_{3L} - 2Q^\gamma \sin^2\theta)\ (j - \frac{k}{2}) \tag{24a}$$

$$g_A^f = - T_{3L} j + \frac{1}{2} (1 + T_{3L})\, k - \frac{1}{4}\, \ell\,, \tag{24b}$$

where

$$j = \frac{M_W^2}{\cos^2\theta} \left(\frac{\cos^2\alpha}{M_Z^2} + \frac{\sin^2\alpha}{M_{\tilde{Z}}^2} \right) \tag{25a}$$

$$k = \frac{M_W^2}{\cos^2\theta} \left(\frac{1}{M_Z^2} - \frac{1}{M_{\tilde{Z}}^2} \right) \frac{\bar{g}}{e} \sin\theta \cos\theta \sin\alpha \cos\alpha \tag{25b}$$

$$\ell = \frac{M_W^2}{\cos^2\theta} \left(\frac{\sin^2\alpha}{M_Z^2} + \frac{\cos^2\alpha}{M_{\tilde{Z}}^2} \right) \left(\frac{\bar{g}}{e} \right)^2 \sin^2\theta \cos^2\theta \quad . \tag{25c}$$

Similarly, in terms of j, k, ℓ,

$$a = (1 - \frac{20}{9} \sin^2\theta)\ (j + k) \tag{26a}$$

$$b = (1 - 4 \sin^2\theta)\ (j - \frac{k}{3}). \tag{26b}$$

Thus all the low energy model independent parameters considered here are simple functions of j, k, ℓ, which are in turn expressed in terms of the sum and the product of the two boson masses.

From eqs. (10) and (25), we obtain

$$j = \frac{\rho + \tilde{\rho} - 1}{\rho\tilde{\rho}} \tag{27a}$$

$$k = \pm \frac{1}{\rho\tilde{\rho}} \left[(\rho + \tilde{\rho} - 1)\ (\rho - 1)\ (1 - \tilde{\rho}) \right]^{\frac{1}{2}} \quad (\pm \text{ for } \varepsilon \lesseqgtr 0) \tag{27b}$$

$$\ell = \frac{\rho + \tilde{\rho} - 1}{\rho\tilde{\rho}} \quad (= j). \tag{27c}$$

From eqs. (5) and (27), in terms of the model parameters,

$$j = \ell = \frac{1}{1 - \varepsilon^2} \tag{28a}$$

$$k = -\frac{\varepsilon}{1 - \varepsilon^2} . \tag{28b}$$

Finally putting eqs. (24), (26), and (28) together, we arrive at the expressions for model independent parameters in terms of the MMM parameters:

$$g_V^e = -\frac{1}{2}(1 - 4\sin^2\theta)\frac{1 + \frac{\varepsilon}{2}}{1 - \varepsilon^2} \tag{29a}$$

$$g_A^e = \frac{1}{4(1 + \varepsilon)} \tag{29b}$$

$$g_V^u = \frac{1}{2}(1 - \frac{8}{3}\sin^2\theta)\frac{1 + \frac{\varepsilon}{2}}{1 - \varepsilon^2} \tag{29c}$$

$$g_A^u = -\frac{3}{4}\frac{1}{1 - \varepsilon} \tag{29d}$$

$$g_V^d = -\frac{1}{2}(1 - \frac{4}{3}\sin^2\theta)\frac{1 + \frac{\varepsilon}{2}}{1 - \varepsilon^2} \tag{29e}$$

$$g_A^d = \frac{1}{4(1 + \varepsilon)} \tag{29f}$$

$$a = (1 - \frac{20}{9}\sin^2\theta)\frac{1}{1 + \varepsilon} \tag{29g}$$

$$b = (1 - 4\sin^2\theta)\frac{1 + \frac{\varepsilon}{3}}{1 - \varepsilon^2} \tag{29h}$$

Expressions for g_V^e, g_A^e, α, β, γ, δ, a, c are listed again in Table 2 and compared with the corresponding expressions in the standard model. Also shown there are the data from various experimental groups compiled by Langacker et al. [26], and the numbers from the best fit to MMM (see next).

(iii) Fitting

First of all, we observe from Table 2 that all the eight parameters considered are independent of A. In the case of no mixing ($\varepsilon = 0$), this is easy to understand; the contribution from the new gauge sector is, in the zero momentum transfer limit, a function of $\frac{\tilde{g}^2}{M_{\tilde{Z}}^2}$, which is independent of $\tilde{g}$ in MMM. Even in the case of non-zero mixing, as mentioned before, all the parameters are functions of j, k, ℓ, which are all independent of A (eqs. (28a,b)). Thus the neutrino reactions and the eD asymmetry impose no constraints on A. Information on the strength of the $\tilde{U}(1)$ coupling will come from $e^+e^- \to \mu^+\mu^-$ at PETRA energies.

Now we proceed to perform a two-parameter fit to data with $\sin^2\theta$ and ε. Fig. 1 (a,b) show the regions in the (ε, $\sin^2\theta$) plane consistent with data within one and a half standard deviation for each model independent parameter. We would like to determine the values of ε and $\sin^2\theta$ as precisely as possible, since they have implications for, among other things, boson masses. The lighter boson mass $M_Z^<$ has an upper bound:

$$\rho^< \leq 1 - \varepsilon^2 , \tag{30a}$$

$$\text{or } M_Z^< \leq \frac{M_W}{\cos\theta} \sqrt{1 - \varepsilon^2} \quad \text{(equality for } A \to \infty\text{)}. \tag{30b}$$

That non-zero mixing (ε) is needed is apparent from the axial coupling for neutrino reactions; for $\varepsilon = 0$, $g_A^e = \frac{1}{4}$, and $\delta = -\frac{1}{2}$, which are more than four standard deviations off. In Fig. 1(a) the horizontal band comes from axial couplings (g_A^e, β, δ) which are independent of $\sin^2\theta$.

To gain a better understanding of the location of the allowed regions in Fig. 1, we consider some special cases of MMM to be compared with the standard model, before we present the best fit to data. For $\varepsilon = -\frac{1}{2}$, neutrino interaction parameters are reduced to their standard model expressions. Indeed, the small shaded region in Fig. 1(a) around $\varepsilon = -\frac{1}{2}$, $\sin^2\theta = .239$ (from the best one-parameter fit to ν data alone [28]) is consistent with all six ν parameters, but not with eD parameters, especially c. The best fit to ν data gives

$$\varepsilon = -.46 \quad \sin^2\theta = .241 .$$

For these values a = .86, c = .90, which are 1.5 σ and 7 σ off, respectively.

On the other hand, for $\varepsilon = 0$ the eD parameters are the same as in the standard model, as they should, since the additional $\tilde{U}(1)$ e and quark currents are purely axial and do not contribute to the asymmetry [29]. Also unchanged are the vector ν parameters (g_V^e, α, γ) and β, for which the isolated axial contribution from $\tilde{U}(1)$ cancels. However, $\varepsilon = 0$, $\sin^2\theta = .224$ (from the best fit to SLAC data [28]) are in gross disagreement with data for axial ν parameters, g_A^e and δ, as mentioned before. From Fig. 1(b) we see that the regions consistent with SLAC data are not restricted to near $\varepsilon = 0$,

but comprises a wide range of ε , including a region around $\varepsilon = -\frac{1}{2}$ where the horizontal ν axial band is located. $\sin^2\theta$ allowed by SLAC data in this region is larger than in the standard model.

Thus it is not surprising that the best fit to all data for MMM gives:

$$\varepsilon = -.44 , \quad \sin^2\theta = .295 . \tag{31}$$

For these values all eight parameters are in good agreement with data, as shown in the last column of Table 2. The relatively large value of $\sin^2\theta$ may not be a problem yet, in view of the absence of a realistic supersymmetric GUT including $\tilde{U}(1)$. The fit is generally improved when we include in Section 3 a Higgs isosinglet transforming non-trivially under $\tilde{U}(1)$.

To get an idea of the location of the boson masses, we note that the best fit (31) gives:

$$\rho^{<} \leq .81 , \tag{32a}$$

$$\text{or} \quad M_z^{<} \leq 73.5 \ \text{GeV} , \tag{32b}$$

while $M_w = 68.7$ GeV. The upper bound corresponds to $A \to \infty$, and as A gets smaller, so does $M_z^{<}$. The lower bound on A, thus on $M_z^{<}$, can possibly come from data for the $\mu^+\mu^-$ forward-backward asymmetry in e^+e^- annihilation, which is considered next.

(iv) Asymmetry in $e^+e^- \to \mu^+\mu^-$

As in most other multi-boson models where there is at least one neutral boson lighter than the standard model Z, we expect the forward-backward asymmetry $A^{\mu\mu}$ to be more negative at low energy than in the standard model. The contributions to the asymmetry come from three interference terms among photon, Z, and $\tilde{Z}$ exchanges [30].

$$A^{\mu\mu} = \frac{3}{4}\,\frac{F_3}{F_1},$$

$$F_1 = 1 + 2\,[g_v^2 \mathrm{Re}(R) + \tilde{g}_v^2 \mathrm{Re}(\tilde{R})] + (g_v^2 + g_A^2)^2 |R|^2$$

$$+ (\tilde{g}_v^2 + \tilde{g}_A^2)^2 |\tilde{R}|^2 + 2\,\mathrm{Re}(R^*\tilde{R})\,(g_v\tilde{g}_v + g_A\tilde{g}_A)^2,$$

$$F_3 = 2\,[g_A^2 \mathrm{Re}(R) + \tilde{g}_A^2 \mathrm{Re}(\tilde{R})] + 4\,[g_v^2 g_A^2 |R|^2 + \tilde{g}_v^2 \tilde{g}_A^2 |\tilde{R}|^2]$$

$$+ 2\,\mathrm{Re}(R^*\tilde{R})\,(g_v\tilde{g}_A + g_A\tilde{g}_v)^2, \qquad (33)$$

where $R = \dfrac{s}{e^2(s - M_Z^2 + i\,M_Z\Gamma)}$, and g_v, g_A are the vector and axial couplings of e (μ) to Z.

For center of mass energy ($\sqrt{s}$) much less than the smaller of the boson masses, the interference between Z and $\tilde{Z}$ exchanges is negligible, and the asymmetry is approximately given by:

$$A^{\mu\mu} = \frac{3}{2}\,(g_A^2\,R + \tilde{g}_A^2\,\tilde{R}), \qquad (34)$$

where the widths have been ignored.

One of the two terms in eq. (34) is expected to be negligible compared to the other, especially when the two masses are widely separated, but the sum results in algebraic simplification.

$$g_A^2 R + \tilde{g}_A^2 \tilde{R} = - \frac{\sigma}{16 \sin^2\theta \cos^2\theta} (j' - 2k' + \ell') , \qquad (35)$$

where

$$j' = - \left(\frac{\cos^2\alpha}{\sigma - \rho} + \frac{\sin^2\alpha}{\sigma - \tilde{\rho}} \right) \qquad (36a)$$

$$k' = \left(\frac{1}{\sigma - \rho} - \frac{1}{\sigma - \tilde{\rho}} \right) \sin\alpha \cos\alpha \sin\theta \cos\theta \frac{\bar{g}}{e} \qquad (36b)$$

$$\ell' = - \left(\frac{\sin^2\alpha}{\sigma - \rho} + \frac{\cos^2\alpha}{\sigma - \tilde{\rho}} \right) \left(\frac{\bar{g}}{e} \right)^2 \sin^2\theta \cos^2\theta , \qquad (36c)$$

$\sigma = \frac{s \cos^2\theta}{M_W^2}$, i.e. center of mass energy squared in units of the standard Z mass squared.

j', k', ℓ' reduce to j, k, ℓ of eqs. (27a,b,c) in the zero limit of center of mass energy:

$\ell' (\sigma = 0) = \ell$, etc.

In terms of the model parameters,

$$j' = \frac{(\rho + \tilde{\rho} - 1) - \sigma}{(\sigma - \rho)(\sigma - \tilde{\rho})} = \frac{A - \sigma}{\sigma^2 - (A + 1)\sigma + A(1 - \varepsilon^2)} \qquad (37a)$$

$$k' = \pm \frac{1}{(\sigma - \rho)(\sigma - \tilde{\rho})} [(\rho + \tilde{\rho} - 1)(\rho - 1)(1 - \tilde{\rho})]^{\frac{1}{2}} \quad (\varepsilon \lessgtr 0)$$

$$= \frac{2 A \varepsilon}{\sigma^2 - (A+1)\sigma + A(1-\varepsilon^2)} \tag{37b}$$

$$\ell' = \frac{(1-\sigma)(\rho + \tilde{\rho} - 1)}{(\sigma - \rho)(\sigma - \tilde{\rho})} = \frac{(1-\sigma) A}{\sigma^2 - (1+A)\sigma + A(1-\varepsilon^2)} . \tag{37c}$$

Putting eqs. (5) and (37) together, we finally have

$$A^{\mu\mu} = -\frac{3\sigma}{32 \sin^2\theta \cos^2\theta} \left\{ \frac{2(1+\varepsilon) - \sigma}{(1-\varepsilon^2) - \sigma} + \frac{1}{(1-\varepsilon^2) - \sigma} \frac{\sigma [(1+\varepsilon) - \sigma]^2}{[(1-\varepsilon^2) - \sigma] A - (\sigma - \sigma^2)} \right\}. \tag{38}$$

The dependence on A is isolated in the second term in braces. For $\sigma \leq \rho$, which includes the region in energy where there are data available and where eq. (38) is approximately valid, this A-dependent term is always positive, regardless of A. Thus $A^{\mu\mu}$ has an upper bound:

$$A^{\mu\mu} \leq -\frac{3\sigma}{32 \sin^2\theta \cos^2\theta} \frac{2(1+\varepsilon) - \sigma}{(1-\varepsilon^2) - \sigma} \quad \text{(equality for } A \to \infty\text{)}. \tag{39}$$

If we compare the expression (39) with $A^{\mu\mu}$ in the standard model:

$$A^{\mu\mu}_{\text{standard}} = -\frac{3}{32 \sin^2\theta \cos^2\theta} \frac{\sigma}{1-\sigma} , \tag{40}$$

we see that for the same value of $\sin^2\theta$, the minimum of $|A^{\mu\mu}|$ in eq. (38) is always greater than $|A^{\mu\mu}_{\text{standard}}|$, for $\sigma \leq 1 - \varepsilon^2$. Thus, even for $A \to \infty$, which corresponds to $M_{\tilde{Z}}$ at infinity, the addition of an extra gauge symmetry with the minimal Higgs structure

implies a more negative value of $A^{\mu\mu}$ than in the standard model at low energy. Also the slope of $A^{\mu\mu}$ as $\sigma \to 0$ (which is independent of A) is steeper in MMM than in the standard model by a factor of $\frac{2}{1 - \varepsilon}$.

For the values of the MMM parameters determined earlier (eq. (31)), and for $\sqrt{s}$ = 34 GeV, eq. (38) becomes

$$A^{\mu\mu} = - (.117 + \frac{.005}{A - .226}). \tag{41}$$

While some experimental groups (CELLO [17], MARK J [18]) reported data consistent with the standard model prediction, other groups (TASSO [19], JADE [20]) find the asymmetry considerably more negative. In the former case, the errors are not small enough to rule out MMM, and A will have a lower bound. In the latter, if we take the TASSO data ($A^{\mu\mu} = - .16 \pm .03$) [19], for example, the bounds on A are:

$$.29 \leq A \leq .61 , \tag{42}$$

which corresponds to

$$43 \text{ GeV} \leq M_{\tilde{z}} \leq 53 \text{ GeV} , \tag{43a}$$

$$85 \text{ GeV} \leq M_z \leq 90 \text{ GeV} . \tag{43b}$$

In Fig. 2 the predictions for $A^{\mu\mu}$ in MMM and in the standard model

are compared. The data from various groups are shown in Fig. 2(b).

3. THE EXTENDED MIXING MODEL (EMM)

(i) Parametrization

While MMM considered in the previous section was shown to be consistent with the existing low-energy data, it could be soon ruled out by data from more asymmetry measurements or the upcoming $p\bar{p}$ collision experiments. In this section an extension of MMM is made in view of the fact that in actual models SU(3) X SU(2) X U(1) singlet Higgs fields ϕ_o^i (i = 1 to N) are often introduced [2,25], which have $\tilde{U}(1)$ charges, $\tilde{y}_o^i$ and obtain non-zero VEV's. These fields have the potential to improve fits to data, since in effect they introduce a new parameter into the neutral current sector. The quantum numbers of ϕ_o^i are listed in Table 1.

The covariant derivative for ϕ_o^i is:

$$D_\mu \phi_o^i = (\partial_\mu - i\, \tilde{y}_o^i\, \tilde{g}\, \tilde{B}_\mu)\, \phi_o^i \ . \tag{1}$$

As ϕ_o^i obtain VEV's, h_o^i, the contribution to the mass matrix from ϕ_o^i is written as:

$$(D_\mu \phi_o^i)^\dagger (D^\mu \phi_o^i) \sim \frac{1}{4} (h_1^2 + h_2^2)\, (t - 1)\, \bar{g}^2\, \tilde{B}_\mu^2 \ , \tag{2}$$

where

$$t = 1 + \sum_i \frac{(\tilde{y}_o^i\, h_o^i)^2}{h_1^2 + h_2^2} \ . \tag{3}$$

The mass matrix then becomes

$$M^2 = \frac{1}{4}(h_1^2 + h_2^2) \begin{bmatrix} g^2 & -gg_2 - g\bar{g}\epsilon \\ -gg_2 & g_2^2 \quad g_2\bar{g}\epsilon \\ -g\bar{g}\epsilon & g_2\bar{g}\epsilon \quad \bar{g}^2 t \end{bmatrix}. \tag{4}$$

Again we have chosen $y_1 = -y_2 = \frac{1}{2}$ not to break electromagnetism. (Otherwise, det $M^2 \propto (y_1 + y_2)^2 \neq 0$, and the photon will develop mass.)

The non-zero eigen values satisfy:

$$\rho + \tilde{\rho} = 1 + At \tag{5a}$$

$$\rho\tilde{\rho} = A(t - \epsilon^2) . \tag{5b}$$

We choose the following solutions to eq. (5) (as $\epsilon \to 0$, $\rho \to 1$ and $\tilde{\rho} \to At$):

$$\rho = \frac{1}{2}\left\{1 + At + (1 - At)\sqrt{1 + \frac{4A\epsilon^2}{(1 - At)^2}}\right\} \tag{6a}$$

$$\tilde{\rho} = \frac{1}{2}\left\{1 + At - (1 - At)\sqrt{1 + \frac{4A\epsilon^2}{(1 - At)^2}}\right\}. \tag{6b}$$

The upper limit of the smaller boson mass is now given by:

$$\rho^< \leq 1 - \frac{\epsilon^2}{t} , \tag{7}$$

which is larger than in MMM for the same value of ϵ.

The expression for the mixing angle α is exactly the same as in MMM in terms of ρ and $\tilde{\rho}$ (eq. (2.10)). The intermediate quantities j, k, ℓ, although they are still the same functions of ρ and $\tilde{\rho}$, are modified since ρ and $\tilde{\rho}$ now depend on t:

$$j = \frac{t}{t - \epsilon^2} \tag{8a}$$

$$k = -\frac{\epsilon}{t - \epsilon^2} \tag{8b}$$

$$\ell = \frac{1}{t - \epsilon^2} \quad . \tag{8c}$$

The eight model independent parameters are now given by:

$$g_V^e = -\frac{1}{2}(1 - 4X)\frac{t + \frac{\epsilon}{2}}{t - \epsilon^2} \tag{9a}$$

$$g_A^e = \frac{1}{2}\frac{t - \frac{1 + \epsilon}{2}}{t - \epsilon^2} \tag{9b}$$

$$\alpha = (1 - 2X)\frac{t + \frac{\epsilon}{2}}{t - \epsilon^2} \tag{9c}$$

$$\beta = -\frac{t + \frac{\epsilon}{2}}{t - \epsilon^2} \tag{9d}$$

$$\gamma = -\frac{2}{3}X\frac{t + \frac{\epsilon}{2}}{t - \epsilon^2} \tag{9e}$$

$$\delta = -\frac{\frac{1}{2} + \epsilon}{t - \epsilon^2} \tag{9f}$$

$$a = \left(1 - \frac{20}{9} X\right) \frac{t - \varepsilon}{t - \varepsilon^2} \tag{9g}$$

$$c = \left(1 - \frac{20}{9} X\right) \frac{t - \varepsilon}{t - \varepsilon^2} + \left(\frac{1}{4} - X\right) \frac{t + \frac{\varepsilon}{3}}{t - \varepsilon^2} , \tag{9h}$$

where $X \equiv \sin^2\theta$.

(ii) Comparison with Low Energy Data

Again the expressions (9) are independent of A as in MMM. For $t = 1$ they reduce to the MMM expressions, as they should. We also notice that for large t the standard model is asymptotically recovered, as in models where the scale of the $\tilde{U}(1)$ breaking is made large compared to O (100) GeV [25]. EMM is truly an extension of the standard model in the sense that there is now a parameter for a certain value of which the standard model is recovered. Therefore, we expect that regardless of the value of ε , a very large value of t will give as good a fit to data as the single-parameter standard model.

In Fig. 3 the regions in the $\varepsilon - t$ plane consistent with neutrino data for $\sin^2\theta$ -independent quantities to within 1.5 σ are shown. Figs. 4 and 5 show, for a representative value of $\sin^2\theta = .230$, the regions in the $\varepsilon - t$ plane consistent with neutrino and eD data for $\sin^2\theta$ -dependent quantities to within 1.5σ and 1σ, respectively. One region consistent with all data, as noted before, lies above a certain large value of t and comprises a wide range (almost all values, for a reasonable value of $\sin^2\theta$) of ε.

Thus it is not surprising that the best fit to all data gives t

of the order of a few hundred, for $\sin^2\theta$ ranging from .220 to .250, which corresponds to $h_o^1 \sim h_{1,2} \times O(10)$, unless N is large. This value of t may seem too large in view of the theoretical prejudice regarding naturalness. However, the value of t is very sensitive to data, and as mentioned before, the current data can be accommodated for a wide range of t (including $t \sim 5$) as well as or better than in the standard model. The present experimental accuracy thus places virtually no useful constraint on the allowed range of t. It should be noted that for smaller t the allowed range of ε becomes more restricted, which has implications for the upper bound on the lower boson mass (see eq. (7)).

As an illustration of these points, we consider the special case $\varepsilon = -\frac{1}{2}$. From Fig. 6 it is seen that a much smaller value of t is permitted than the best fit. Indeed we observe from eqs. (9) that for $\varepsilon = -\frac{1}{2}$ all the ν parameters are reduced to their standard model expressions, just as in MMM. eD parameters in this case are still functions of both $\sin^2\theta$ and t. This t-dependence will serve as the basis for an improved fit to eD data with the other parameters (ε, $\sin^2\theta$) determined from ν data as in the standard model. In this respect, this model (with $\varepsilon = -\frac{1}{2}$, and $\sin^2\theta$ and t as free parameters) resembles the SU(2) X U(1) X U(1) model of Deshpande and Iskandar [31] whose ν sector is the same as the standard model, and whose electron-quark reactions are described by an additional parameter. For $\varepsilon = -\frac{1}{2}$ and $\sin^2\theta = .239 \pm .010$ (from the standard model fit to ν data) the best fit to eD data gives

$$t = 7.85 \begin{matrix} + 12.9 \\ - 3.35 \end{matrix} .$$

Fig. 6 shows regions in the $\sin^2\theta$ - t plane consistent with data for a and c within 1 σ. Again it is clear that t is highly sensitive to data.

Another special case where some low-energy parameters are the same as in the standard model results for $\varepsilon = 0$. As in MMM, the eD parameters and also g_V^e, α, β, γ are unchanged, but g_A^e and δ now depend on t. The best fit to data for these two parameters gives $t \tilde{=} 350$, which makes $\varepsilon = 0$ less favorable than $\varepsilon = -\frac{1}{2}$. ($g_A^e$ tends to favor large t for $\varepsilon = 0$).

To get an idea of the boson masses in EMM, we note from

$$\varepsilon = -\frac{1}{2},\ \sin^2\theta = .239,\ t = 7.85 \qquad (10)$$

we get

$$\rho^{<} \leq .97 , \qquad (11a)$$

or $$M_z^{<} \leq 86.1 \text{ GeV} . \qquad (11b)$$

(iii) Asymmetry in $e^+e^- \to \mu^+\mu^-$

The expression for $A^{\mu\mu}$ is the same as in MMM in terms of j′, k′, ℓ′ (eq. (2.35)). However, j′, k′, ℓ′ are modified:

$$j' = \frac{At - \sigma}{\sigma^2 - (1 + At)\,\sigma + A\,(t - \varepsilon^2)} \qquad (12a)$$

$$k' = -\frac{A\,\varepsilon}{\sigma^2 - (1 + At)\,\sigma + A\,(t - \varepsilon^2)} \qquad (12b)$$

$$\ell' = \frac{(1-\sigma)\,A}{\sigma^2 - (1+At)\,\sigma + A\,(t-\varepsilon^2)} \quad . \tag{12c}$$

Thus from eqs. (2.34), (12), the asymmetry is given by:

$$A^{\mu\mu} = -\frac{3\,\sigma}{32\,\sin^2\theta\,\cos^2\theta}\left\{\frac{(1+t+2\varepsilon)-\sigma}{t\,(1-\sigma)-\varepsilon^2} + \frac{\sigma\,[\sigma-(1+\varepsilon)]^2}{t\,(1-\sigma)-\varepsilon^2}\;\frac{1}{[t\,(1-\sigma)-\varepsilon^2]\,A-(\sigma-\sigma^2)}\right\}. \tag{13}$$

The first term in braces in eq. (13) is again always positive for $\sigma \leq 1 - \frac{\varepsilon^2}{t}$, and smaller than the corresponding term in the MMM prediction for the same value of ε. Since the second term is always positive regardless of A as in MMM, the minimum of $|A^{\mu\mu}|$ in EMM is smaller than that in MMM for same ε, in the range of σ where eq. (13) is approximately valid.

In fitting EMM parameters to the asymmetry data, one must be careful unless t is small ($t \lesssim 5$, which could be too small in view of naturalness). If one works with fairly large t (as required, for example, from the low energy data), the approximation for $A^{\mu\mu}$ in eq. (2.34) may not be valid for asymmetry data considerably larger than predicted in the standard model. This is illustrated in the example given before (eq. (10)). Using the TASSO data ($A^{\mu\mu} = -.16 \pm .03$), we find

$$.020 \leq A \leq .021\,, \tag{14}$$

which corresponds to

$$34 \text{ GeV} \leq M_{\tilde{z}} \leq 35 \text{ GeV} , \tag{15a}$$

$$87 \text{ GeV} \leq M_{\tilde{z}} \leq 88 \text{ GeV} . \tag{15b}$$

For this value of $M_{\tilde{z}}$, the terms neglected in eq. (2.34) are actually bigger than the lowest order terms in eq. (2.34), and should obviously be included for the precise determination of the boson masses. However, the crucial point here is that the location of the lower boson mass is very near the center of mass energy, which is in clear contradiction with, for example, the current data for the e^+e^- total cross section [32].

Why this happens for not so small t and large $| A^{\mu\mu} |$ is seen from the approximation of eq. (13) for large t:

$$A^{\mu\mu} \sim A^{\mu\mu}_{\text{standard}} + (\text{const}) \frac{\sigma[(1 + \varepsilon) - \sigma]^2}{t}$$

$$X \frac{1}{t (1 - \sigma) A - (\sigma - \sigma^2)} , \tag{16}$$

or

$$A \sim \frac{(\text{const})'}{t^2 \Delta} + \frac{\sigma}{t} , \tag{17}$$

where Δ is the deviation from the standard model prediction. For large t, unless Δ is small $A \sim \frac{\sigma}{t}$ regardless of the value of Δ, and A is determined so that the mass of the lighter boson is close to the center of mass energy. Thus it follows that if the asymmetry data considerably larger than the standard model prediction are not

accompanied by the corresponding peak in the e^+e^- total cross-section, t should be small for EMM to be consistent. If small t is indeed preferred, large mixing (ε), in turn, could put a non-trivial upper bound on the lower boson mass (see eq. (7)). To make more definite remarks on the fate of EMM, we would have to wait for more data on $A^{\mu\mu}$ and results from $p\bar{p}$ experiments.

4. OTHER PROCESSES

Two other neutral current processes which are potentially affected by the presence of a new $\tilde{U}(1)$ gauge group are considered in this section.

(i) Widths of Z and $\tilde{Z}$

The decay widths of neutral bosons may soon be directly measured in the upcoming $p\bar{p}$ and e^+e^- experiments. The partial width at the tree level (Γ_o) of a neutral boson Z is easily expressed in terms of the Zf_1f_2 couplings [33].

$$\Gamma_o (Z \to f_1\bar{f}_2) = \frac{M_z}{12\pi} \left[\left(1 - \frac{M_1^2 + M_2^2}{M_z^2}\right)^2 - 4\frac{M_1^2 M_2^2}{M_z^4}\right]^{\frac{1}{2}}$$
$$\times \left\{(g_v^2 + g_A^2)\left[1 - \frac{M_1^2 + M_2^2}{2M_z^2} - \frac{1}{2}\left(\frac{M_1^2 - M_2^2}{M_z^2}\right)^2\right]\right.$$
$$\left. + 3(g_v^2 - g_A^2)\frac{M_1 M_2}{M_z^2}\right\}, \qquad (1)$$

where $M_{1,2}$ are the masses of $f_{1,2}$ and the fermion current used is $\bar{f}_1 \gamma_\mu (g_v + g_A \gamma_5) f_2$.

For most fermions masses are negligible, and eq. (1) simplifies to:

$$\Gamma_o = \frac{M_z}{12\pi} (g_v^2 + g_A^2) . \tag{2}$$

Using the couplings derived in Section 2, and summing over e, ν, u_i, d_i (i:color), we obtain the total widths:

$$\Gamma_o^z = N \frac{M_z}{12\pi} \left[\frac{e^2}{\sin^2\theta \cos^2\theta} \cos^2\alpha \ (1 - 2\sin^2\theta + \frac{8}{3}\sin^4\theta) \right.$$

$$\left. + \frac{15}{32} \bar{g}^2 \sin^2\alpha \right] , \tag{3a}$$

$$\Gamma_o^{\tilde{z}} = N \frac{M_{\tilde{z}}}{12\pi} \left[\frac{e^2}{\sin^2\theta \cos^2\theta} \sin^2\alpha \ (1 - 2\sin^2\theta + \frac{8}{3}\sin^4\theta) \right.$$

$$\left. + \frac{15}{32} \bar{g}^2 \cos^2\alpha \right] , \tag{3b}$$

for N generations.

For the values of ε and $\sin^2\theta$ from the best MMM fit (eq. (2.31)) and A determined from the TASSO data [19] (eq. (2.42)), we obtain

$$\Gamma_o^z \cong 1.8 \text{ GeV} \tag{4a}$$

$$\Gamma_o^{\tilde{z}} \cong .3 \text{ to } .7 \text{ GeV} , \tag{4b}$$

for three generations.

For EMM, since the values of the model parameters were not determined we merely note one special case ($\varepsilon = 0$) where the ratio of the widths simplifies:

$$\frac{\Gamma_o^{\tilde{z}}}{\Gamma_o^{z}} = \frac{15}{32} \frac{1}{(1 - 2\sin^2\theta + \frac{8}{3}\sin^4\theta)} A^{\frac{3}{2}} \sqrt{t} \,. \qquad (5)$$

(ii) The Anomalous Magnetic Moment of the Muon

The weak current contribution to $a_\mu = \frac{g-2}{2}$ in the standard model is known to be too small to detect at the present level of experimental accuracy [34]. We examine here how the addition of $\tilde{U}(1)$ alters this situation.

To lowest order, the weak corrections to a_μ come from the four diagrams in Fig. 7, i.e., one-loop diagrams involving the exchange of $W^{\pm}$, Z, $\tilde{Z}$, and Higgs. As in the standard model calculation, the Higgs contribution is down by $O\left(\frac{M_\mu^2}{M_H^2}\right)$ and will be ignored. The contribution from the charged weak current is the same as in the standard model:

$$a_\mu^{W} = \frac{5}{12\sqrt{2}\pi^2} M_\mu^2 G_F \,. \qquad (6)$$

The contribution from the Z exchange (Fig. 7(b)) is given by [34]:

$$a_\mu^{z} = \frac{M_\mu^2}{12\pi^2}\left\{\left(\frac{Q_V^z}{M_z}\right)^2 - 5\left(\frac{Q_A^z}{M_z}\right)\right\}^2 \,. \qquad (7)$$

$a_\mu^{\tilde{z}}$ is given similarly. The sum of a_μ^{z} and $a_\mu^{\tilde{z}}$ simplifies in terms of the intermediate parameters j, k, ℓ defined in eqs. (3.8):

$$a_\mu^{Z,\tilde{Z}} = \frac{M_\mu^2 G_F}{24\sqrt{2}\pi^2}\left\{[(1 - 4\sin^2\theta)^2 - 5]\, j - 10\, k - 5\, \ell\right\} \,. \qquad (8)$$

Putting eqs. (3.8) and (8) together, the total weak contribution to a_μ in terms of the model parameters is:

$$a_\mu^{\text{weak}} = \frac{M_\mu^2 G_F}{24\sqrt{2}\pi^2}\left\{10 + \frac{1}{t - \varepsilon^2}[(1 - 4\sin^2\theta)\, t - 5\,(1 + t - 2\varepsilon)]\right\} \qquad (9)$$

The current experimental bounds on a_μ^{weak} are:

$$-1.5 \cdot 10^{-8} \leq a_\mu^{weak} \leq 2 \cdot 10^{-8} \text{ [34]}. \qquad (10)$$

For EMM no useful bound on t is obtained, again because of the sensitivity of t to experimental errors. For MMM, in a wide range of ϵ including the best fit from low energy data, eq. (9) is more negative and cancels more of the charged weak current contribution of eq. (6) (which has the opposite sign), to make eq. (9) even smaller than in the standard model. Thus no useful constraints on the model parameters are obtained from the current data for the muon anomalous magnetic moment.

5. SUMMARY AND CONCLUSIONS

In this chapter, the neutral current sector of a class of supersymmetric SU(2) X U(1) X $\tilde{U}$(1) models has been parametrized by A, ϵ, and t, which measure the relative strength of the new $\tilde{U}$(1) interactions, the mixing between the two massive neutral bosons, and the Higgs isosinglet contribution to the boson masses, respectively, in addition to the usual $\sin^2\theta$. Neutral current data including (I) various neutrino interactions, (II) SLAC eD asymmetry, and (III) $\mu^+\mu^-$ forward-backward asymmetry in e^+e^- annihilation have been used to obtain bounds on the two neutral boson masses. (I) and (II) were used to fit $\sin^2\theta$, ϵ, and t, and from (III) bounds on A were obtained.

In the absence of Higgs isosinglets (t = 1; MMM), (I) prefers $\epsilon = -\frac{1}{2}$ while (II) reduces to the standard model expressions for $\epsilon = 0$. The best fit to both (I) and (II) gives $\epsilon = -.44$

and $\sin^2\theta = .295$, for which agreement with the data is good for all the model-independent low-energy parameters considered. The large mixing (both ϵ and $\sin^2\theta$) required in MMM places the upper bound of 74 GeV on the mass of the lighter boson. There is some uncertainty in the current experimental situation for (III). Depending on which asymmetry data we take, the prediction for the lower boson mass can be as low as 43 GeV. (The TASSO data, which are considerably larger than the standard model predicts, give $.29 \leq A \leq .61$ or 43 GeV $\leq M_{\tilde{z}} \leq 53$ GeV.) If a neutral boson does not turn up in the upcoming $p\bar{p}$ experiments until around 90 GeV, MMM is probably ruled out.

If there are Higgs isosinglets present ($t \neq 1$; EMM), as $\epsilon \to \infty$ the standard model is recovered. For a wide range of t (especially for large t) the data for (I) and (II) are well accommodated. Even for not so large t ($t \sim 5$, which is preferred by the theoretical prejudice regarding naturalness), there are regions in the $\epsilon - \sin^2\theta$ plane consistent with (I) and (II). Since the value of t is extremely sensitive to the experimental errors, however, no useful constraints on t are obtained from (I) and (II). As for (III), if the asymmetry is indeed much larger than the standard model prediction, the isosinglet contribution to the boson masses should not dominate. This further implies that the mixing (ϵ) would have to be small if a low-mass boson is not found. On the other hand, if the asymmetry is not large, EMM survives for a wide range of t, regadless of the location of the lighter boson.

More precise low-energy data, the direct production of one or more neutral bosons, or more theoretical constraints will obviously

shed more light on the relevance of the supersymmetric extra $\tilde{U}(1)$ models considered here.

Table 1: Quantum Numbers of the Left-handed Chiral Fields in EMM

	SU(3)	$SU(2)_L$	U(1)	$\tilde{U}(1)$
Q_L	3	2	$\frac{1}{6}$	$\frac{\tilde{y}}{2}$
$\bar{U}_R$	3	1	$\frac{1}{3}$	$\frac{\tilde{y}}{2}$
$\bar{D}_R$	3	1	$-\frac{2}{3}$	$\frac{\tilde{y}}{2}$
L_L	1	2	$-\frac{1}{2}$	$\frac{\tilde{y}}{2}$
$\bar{E}_R$	1	1	1	$\frac{\tilde{y}}{2}$
ϕ_1	1	2	$\frac{1}{2}$	$\tilde{y}$
ϕ_2	1	2	$-\frac{1}{2}$	$\tilde{y}$
ϕ_o^i	1	1	0	$\tilde{y}_o^i$

Table 2: $X \equiv \sin^2\theta$

Model Independent Parameters	MMM	Standard Model	Data	MMM Best Fit
g_V^e	$-\frac{1}{2}(1-4X)\frac{1+\frac{\varepsilon}{2}}{1-\varepsilon^2}$	$-\frac{1}{2}(1-4X)$	$.06 \pm .08$	.09
g_A^e	$\frac{1}{4}\frac{1}{1+\varepsilon}$	$\frac{1}{2}$	$.52 \pm .06$	.45
α	$(1-2X)\frac{1+\frac{\varepsilon}{2}}{1-\varepsilon^2}$	$1-2X$	$.589 \pm .067$	.396
β	$-\frac{1+\frac{\varepsilon}{2}}{1-\varepsilon^2}$	-1	$-.937 \pm .062$	$-.967$
γ	$-\frac{2}{3}X\frac{1+\frac{\varepsilon}{2}}{1-\varepsilon^2}$	$-\frac{2}{3}X$	$-.273 \pm .081$	$-.190$
δ	$-\frac{\frac{1}{2}+\varepsilon}{1-\varepsilon^2}$	0	$-.101 \pm .093$	$-.074$
a	$(1-\frac{20}{9}X)\frac{1}{1+\varepsilon}$	$1-\frac{20}{9}X$	$.60 \pm .16$	.62
c	$(1-\frac{20}{9}X)\frac{1}{1+\varepsilon} + (\frac{1}{4}-X)\frac{1+\frac{\varepsilon}{3}}{1-\varepsilon^2}$	$\frac{5}{4}-\frac{29}{9}X$	$.53 \pm .05$	.57

FIGURE CAPTIONS

Fig. 1(a) Regions in the $\varepsilon - \sin^2\theta$ plane consistent with neutrino data for the parameters g_A^e, α, β, γ, δ to within one and a half standard deviations. The small shaded area is common to all regions. (The region for g_V^e is not shown, which also includes the shaded area.)

(b) Regions in the $\varepsilon - \sin^2\theta$ plane consistent with data for SLAC eD parameters, a (shaded) and c to within one and a half standard deviations.

(c) Regions allowed by (I) neutrino data (Fig. 1(a)) and (II) eD data (Fig. 1(b)) are shown again along with the best fit to MMM.

Fig. 2(a) Predictions for $A^{\mu\mu}$ in the standard model and in MMM for $A \to \infty$.

(b) The shaded region is allowed by MMM and the solid line corresponds to the minimum $|A^{\mu\mu}|$. Also shown are the data from various groups.

Fig. 3 Regions in the $\varepsilon - t$ plane allowed by neutrino data for $\sin^2\theta$ independent parameters to within one and a half standard deviations. The shaded area is common to all regions.

Fig. 4 The shaded region is allowed by ν data for $\sin^2\theta$-dependent parameters to within 1.5 σ, for $\sin^2\theta = .230$.

Fig. 5 The shaded region is allowed by SLAC data to within 1σ for $\sin^2\theta = .230$.

Fig. 6 The shaded region in the $\sin^2\theta$ - t plane is allowed by eD data to within 1 σ for EMM with $\varepsilon = -\frac{1}{2}$. The best fit for t as a function of $\sin^2\theta$ is also shown.

Fig. 7 Diagrams contributing to the weak corrections to a_μ .

REFERENCES

[1] For a review and a list of early references, see P. Fayet and S. Ferrara, Supersymmetry, Phys. Rep. 32 C, 249 (1977).

[2] L. J. Hall and I. Hinchliffe, Phys. Lett. 112 B, 351 (1982) and references contained therein.

[3] For a review, see, for example, P. Langacker, Phys. Rep. 72 C, 185 (1981).

[4] S. Glashow, Nucl. Phys. 22, 579 (1961); S. Weinberg, Phys. Rev. Lett. 19, 1264 (1967); A. Salam, in 8th Nobel Symp. ed., N. Svartholm, pg. 367 (1968).

[5] J. Wess and B. Zumino, Phys. Lett. 49 B, 52 (1974); J. Iliopoulos and B. Zumino, Nucl. Phys. B 76, 310 (1974); S. Ferrara, J. Illiopoulos and B. Zumino, Nucl. Phys. B 77, 413 (1974).

[6] R. N. Cahn, I. Hinchliffe and L. J. Hall, Phys. Lett. 109 B, 426 (1982).

[7] S. Dimopoulos and H. Georgi, Nucl. Phys. B 193, 150 (1981); L. Girardello and M. T. Grisaru, Nucl. Phys. B 194, 65 (1982).

[8] P. Fayet, Phys. Lett. 69 B, 489 (1977); 70 B, 461 (1977).

[9] S. Weinberg, HUTP-81/A047 (1981).

[10] P. Fayet, Phys. Lett. 95 B, 285 (1980); 96 B, 83 (1980).

[11] N. G. Deshpande and R. J. Johnson, Oregon Preprint, OTIS-188 (1982), and references contained therein.

[12] See, for example, E. H. deGroot, G. J. Gounaris, and D. Schildknecht, Phys. Lett. 85 B, 399 (1979).

[13] T. Rizzo and G. Senjanovic, Phys. Rev. D 24, 704 (1981).

[14] The data used here are from the following review articles: J. E. Kim, P. Langacker, M. Levine and H. H. Williams, Rev. Mod. Phys. 53, 211 (1981); P. Q. Hung and J. J. Sakurai, Ann. Rev. Nucl. Part. Sci. 31, 375 (1981).

[15] C. Y. Prescott et al., Phys. Lett. 77 B, 347 (1978); 84 B, 524 (1979).

[16] For the standard model case, see CERN Report 76-18.

[17] CELLO Collab., DESY 82-019.

[18] MARK J Collab., MIT Technical Report #124 (1982).

[19] TASSO Collab., DESY 82-002.

[20] JADE Collab., DESY 81-072.

[21] S. Ferrara, L. Girardello and F. Palumbo, Phys. Rev. D 20, 403 (1979).

[22] P. Fayet, Phys. Lett. 84 B, 416 (1979).

[23] M. Suzuki, Phys. Lett. 115 B, 40 (1982).

[24] J. Ellis and D. V. Nanopoulos, Phys. Lett. 110 B, 44 (1982).

[25] R. Barbieri, S. Ferrara and D. V. Nanopoulos, CERN preprint, TH-3226 (1982); R. Barbieri, S. Ferrara, D. V. Nanopoulos and K. S. Stette, CERN preprint TH-3243 (1982).

[26] H. Georgi and S. Weinberg, Phys. Rev. D 17, 275 (1978).

[27] P. Q. Hung and J. J. Sakurai, ref. 14.

[28] J. Kim et al., ref. 14.

[29] R. N. Cahn and F. J. Gilman, Phys. Rev. D 17, 1313 (1978), and references contained therein.

[30] Proc. LEP Summer Study, CERN 79-01 (1979).

[31] N. G. Deshpande and D. Iskandar, Phys. Lett. 87 B, 383 (1979).

[32] TASSO Collab., DESY 82-010; CELLO Collab., DESY 82-019.

[33] D. Albert et al., Nucl. Phys. B 166, 460 (1980).

[34] J. P. Leveille, Nucl. Phys. B 137, 63 (1978), and references contained therein.

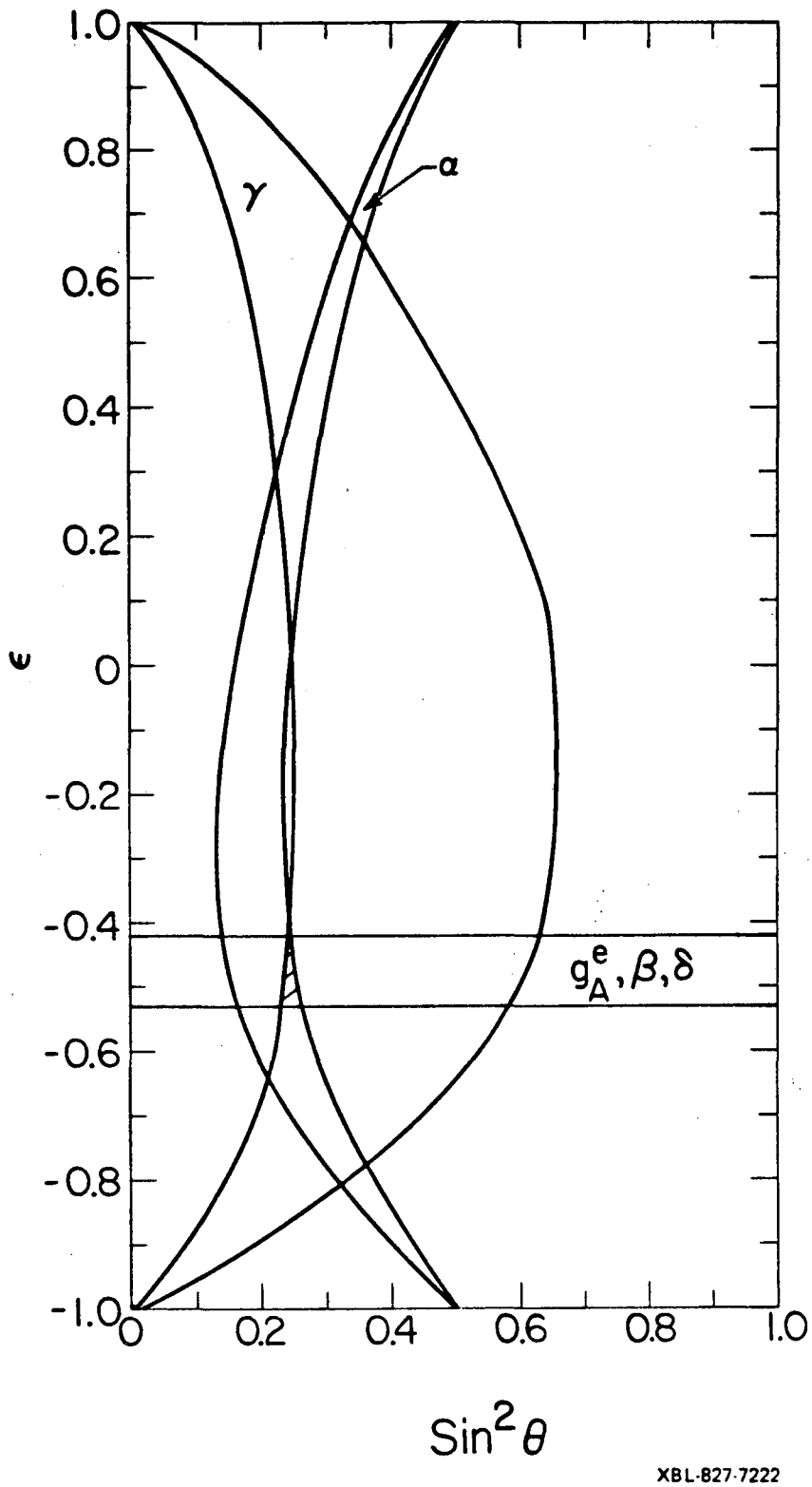
1.0
0.8
0.6
0.4
0.2
0
-0.2
-0.4
-0.6
-0.8
-1.0
ε
γ
α
g_A^e, β, δ
0
0.2
0.4
0.6
0.8
1.0
$\mathrm{Sin}^2\theta$
XBL-827-7222

FIG. 1A

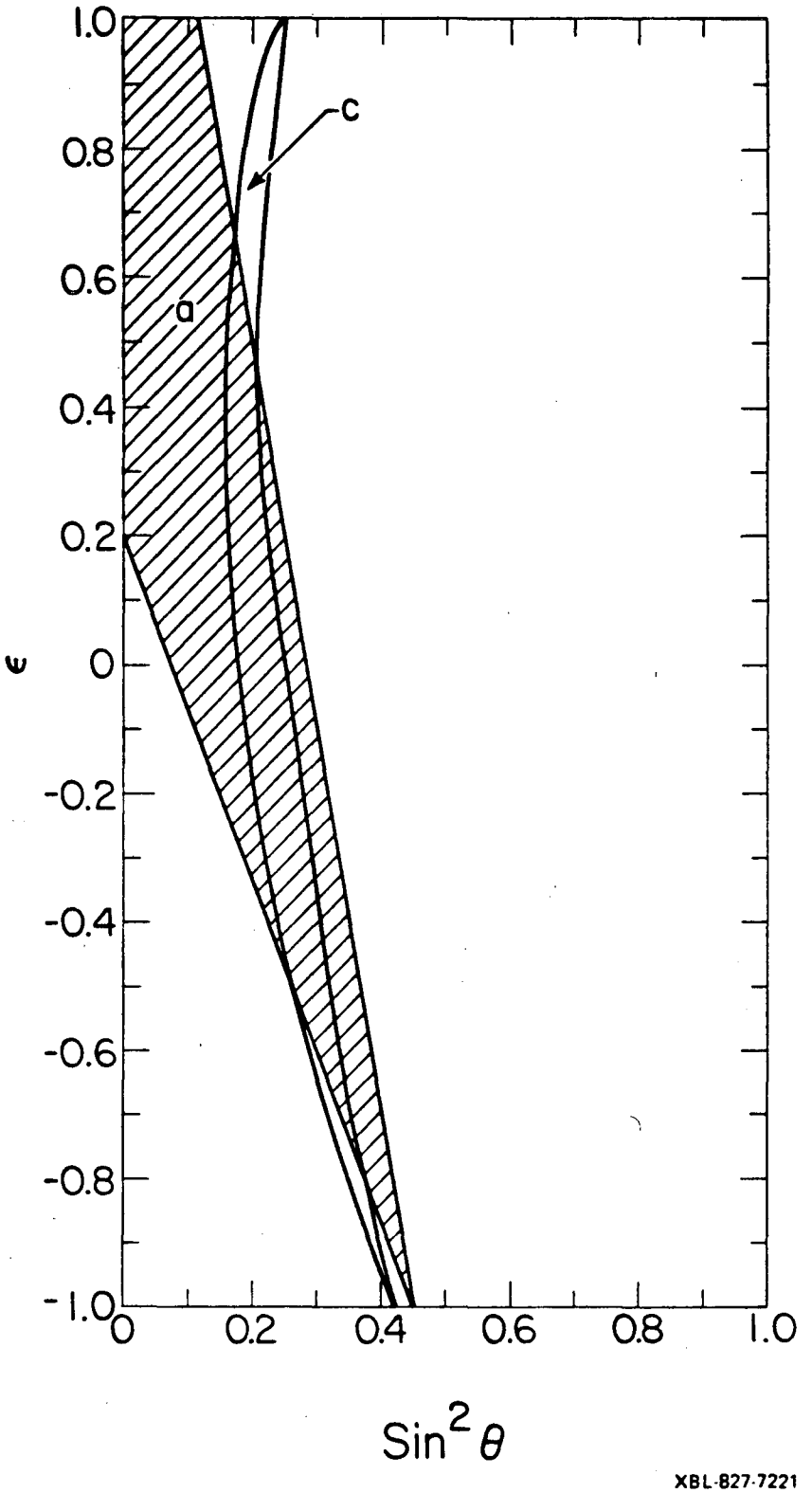
1.0
0.8
0.6
0.4
0.2
0
-0.2
-0.4
-0.6
-0.8
-1.0
ε
a
c
0
0.2
0.4
0.6
0.8
1.0
Sin$^2\theta$
XBL-827-7221

FIG. 1B

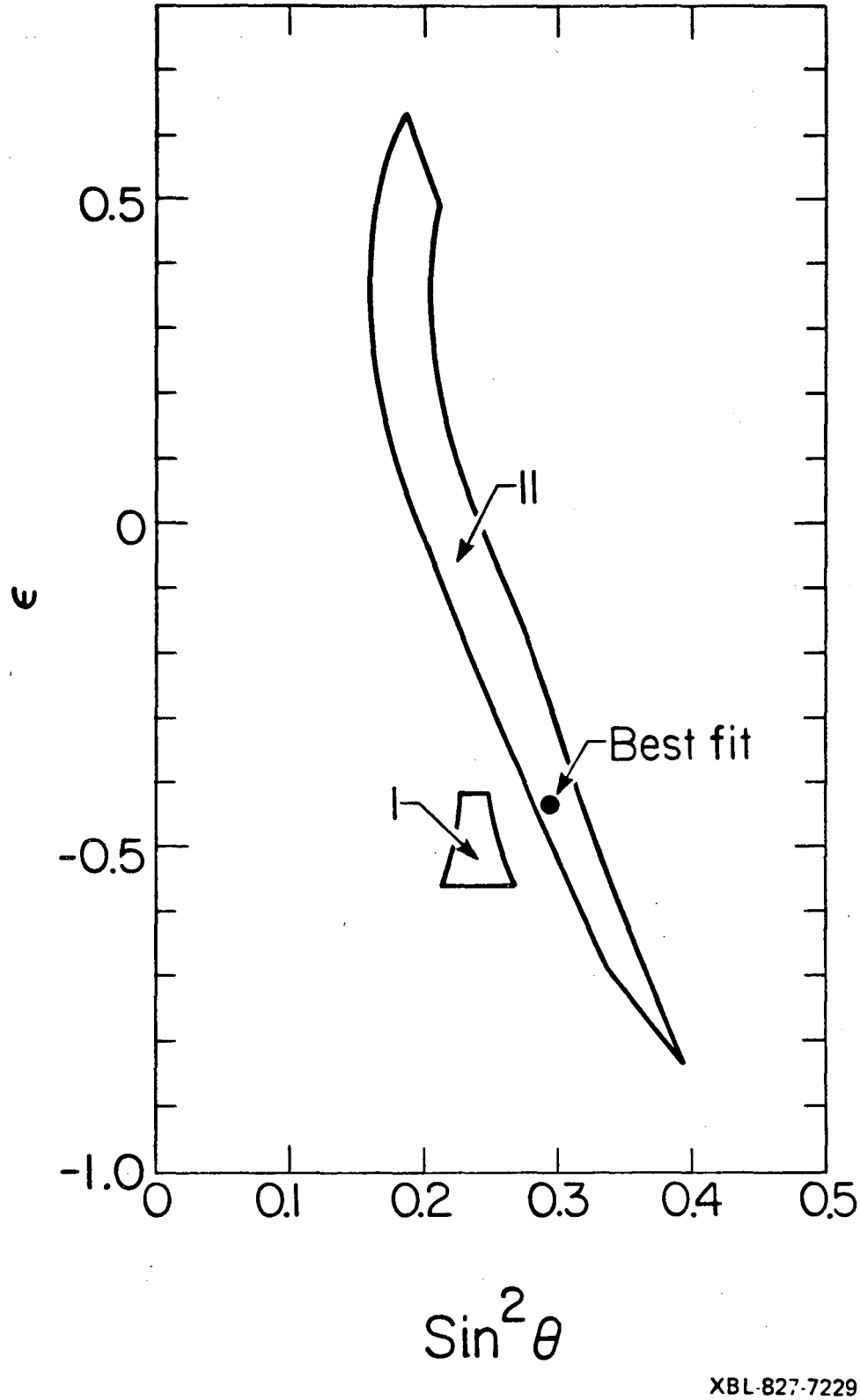

FIG. 1c

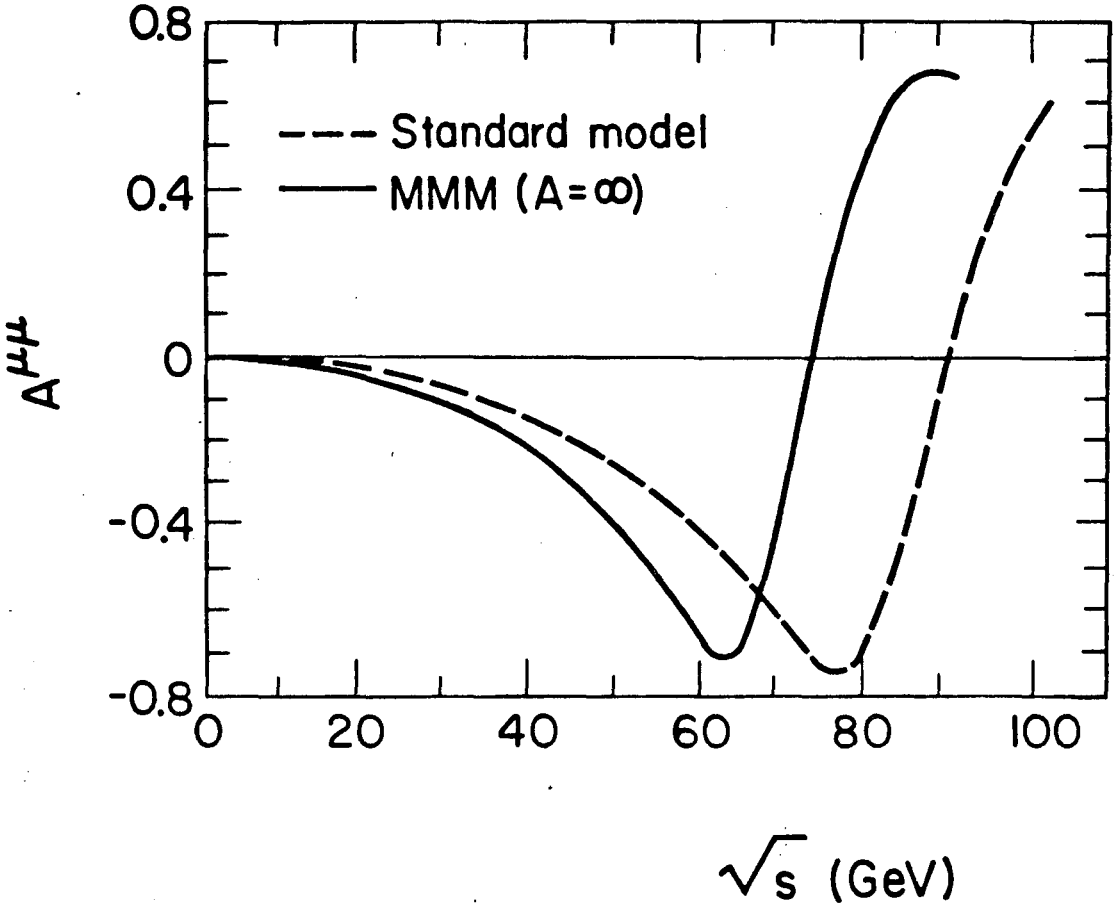

XBL-827-7225

FIG. 2A

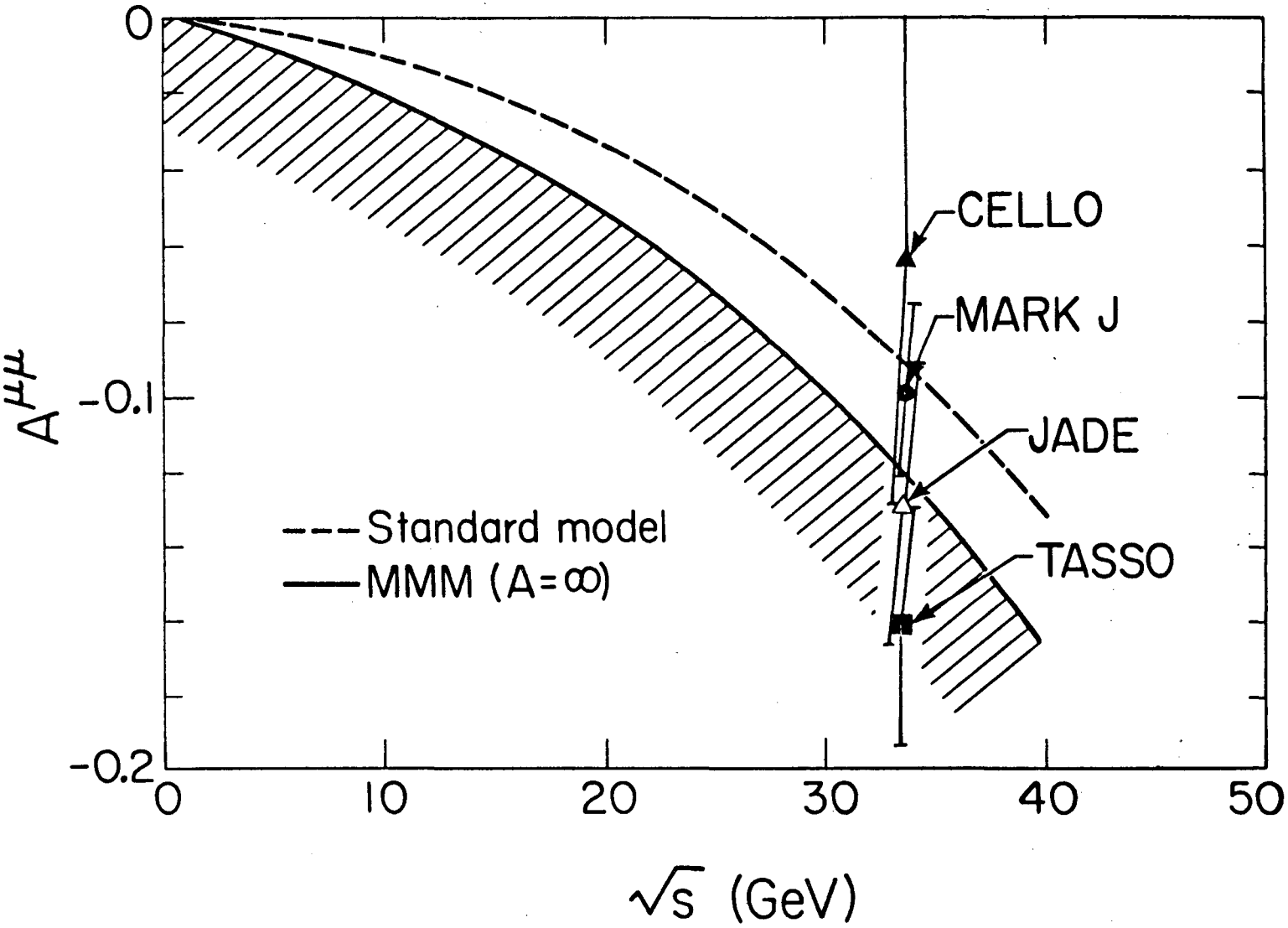
0
-0.1
-0.2
$A^{\mu\mu}$
0
10
20
30
40
50
$\sqrt{s}$ (GeV)
CELLO
MARK J
JADE
TASSO
Standard model
MMM (A=∞)
XBL-827-7224

FIG. 2B

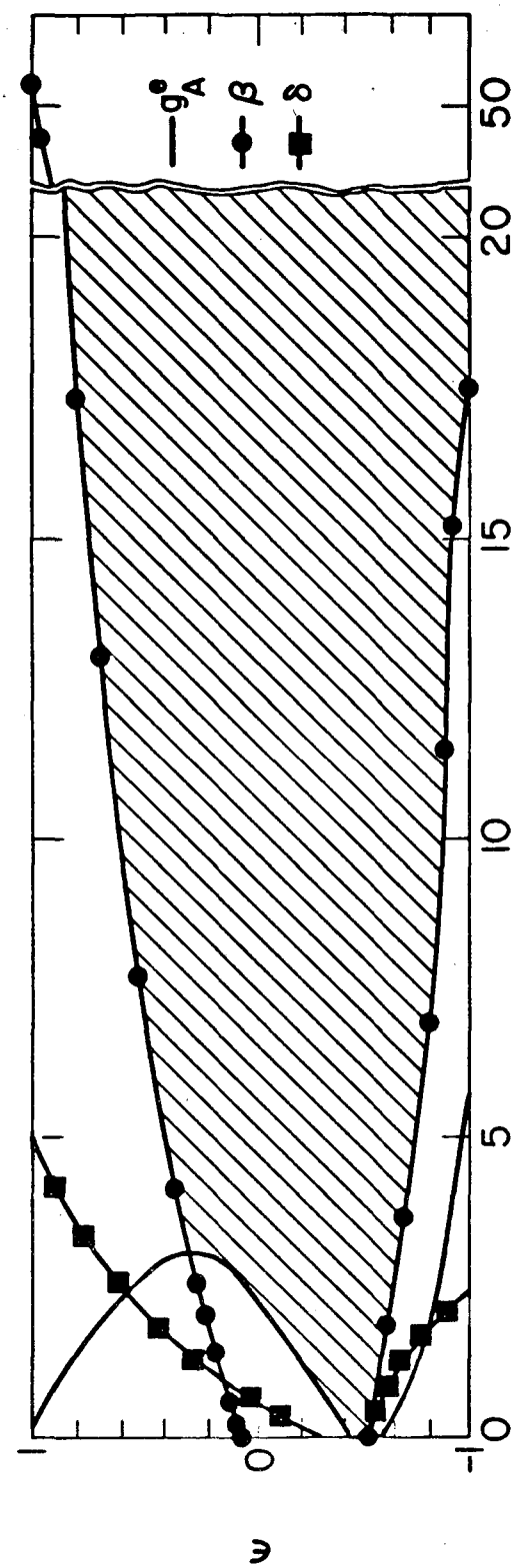

XBL-827-7227

FIG. 3

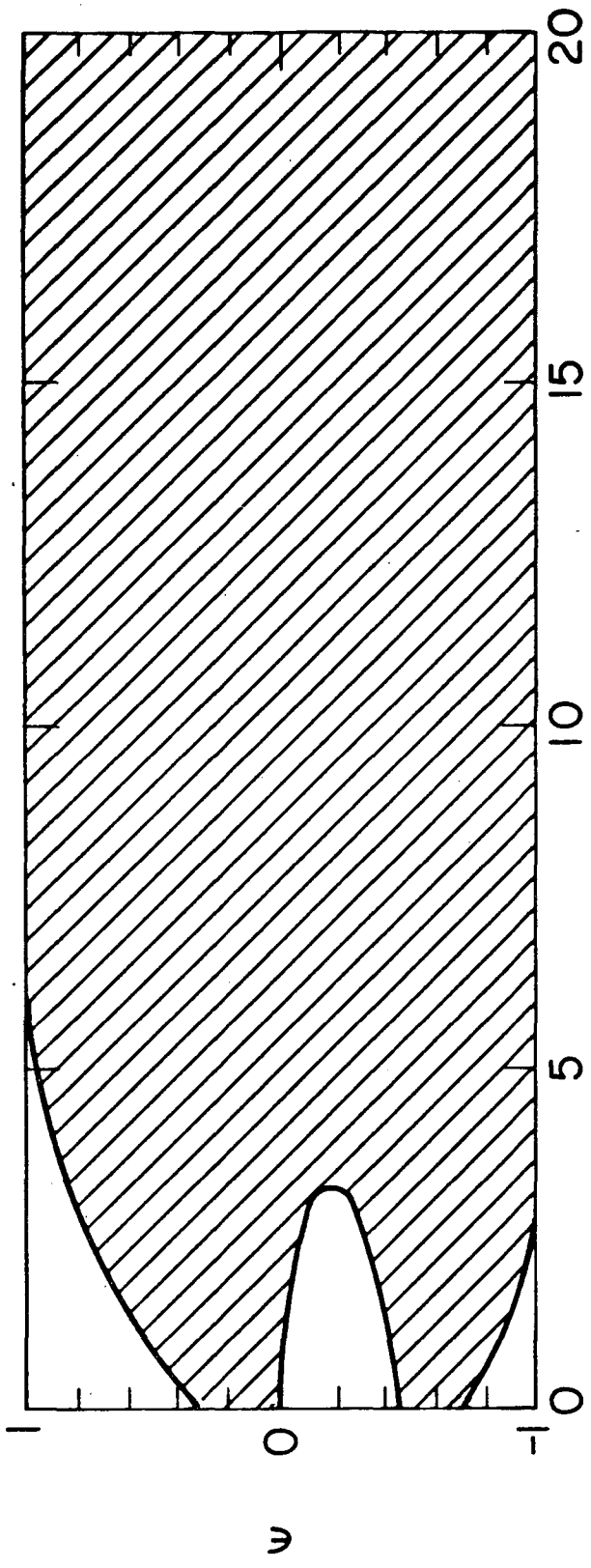

XBL-827-7228

FIG. 4

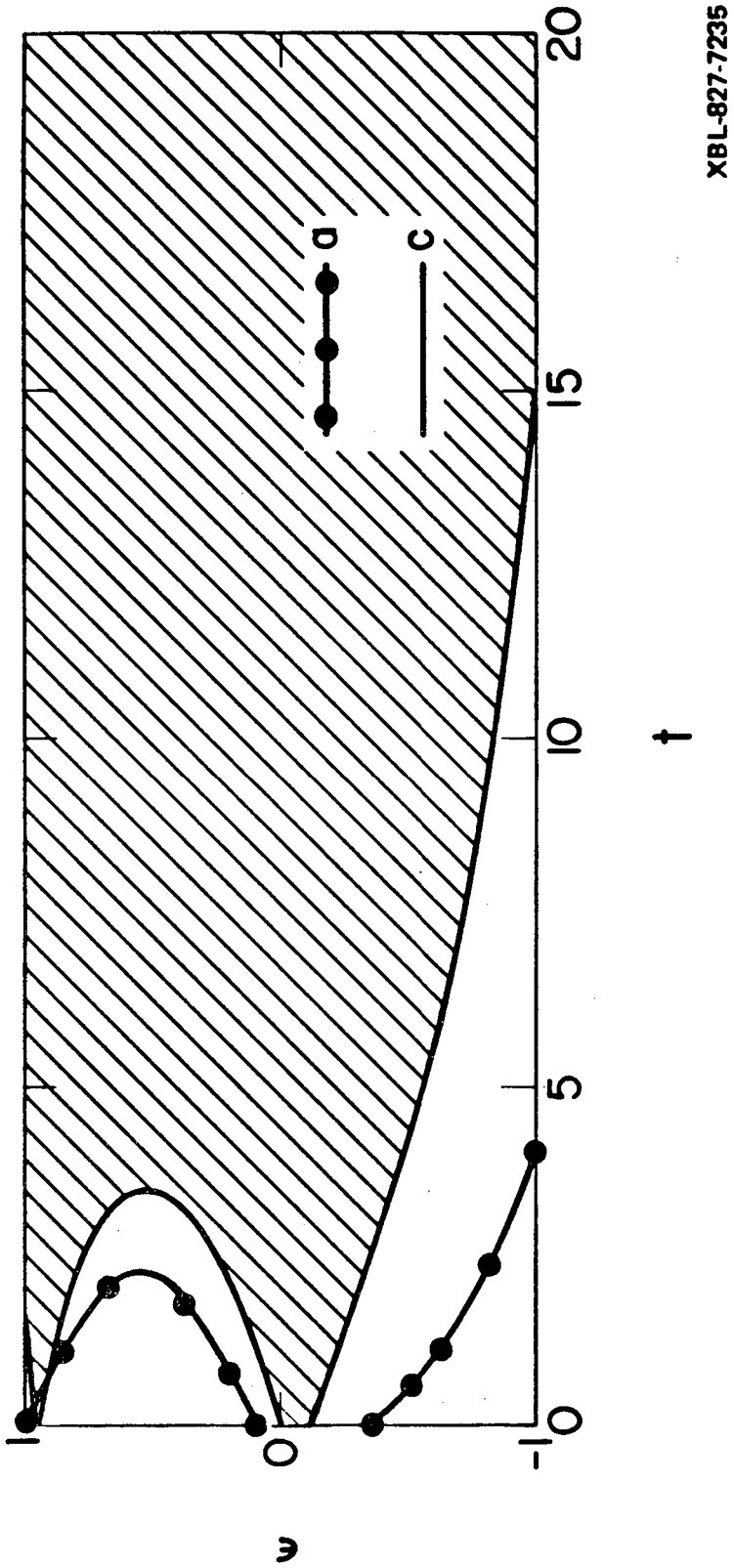

XBL-827-7235

FIG. 5

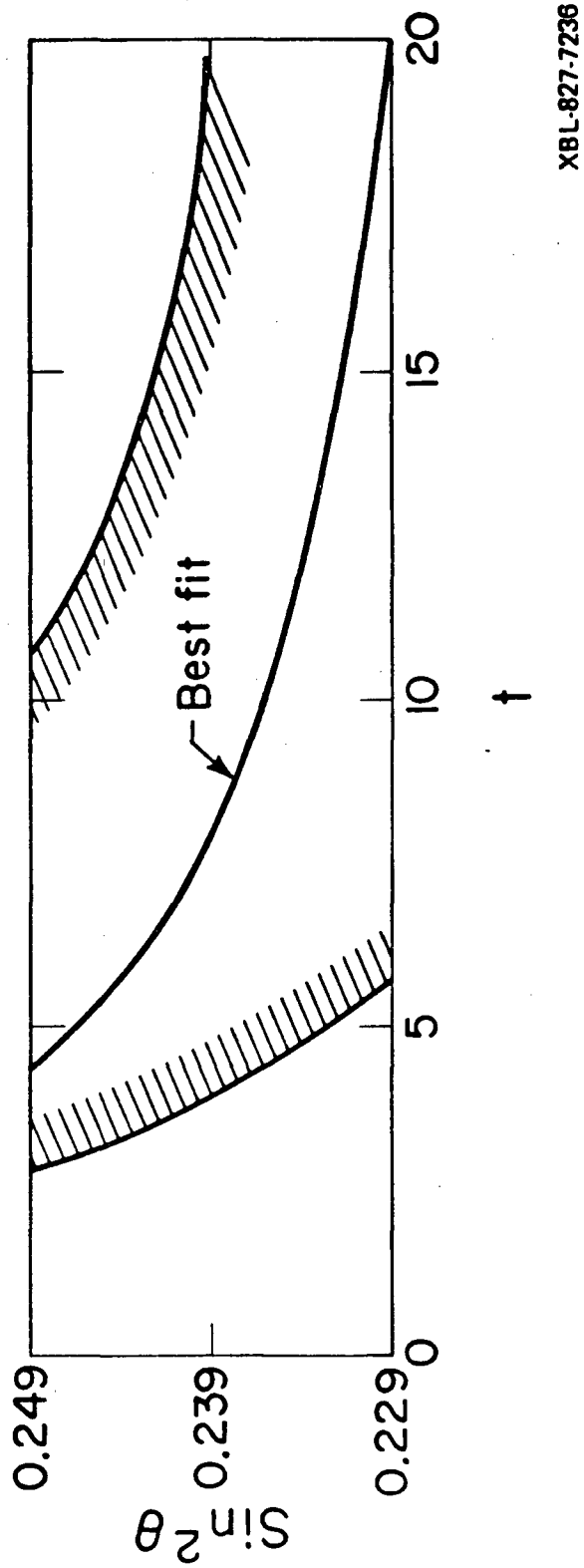

FIG. 6

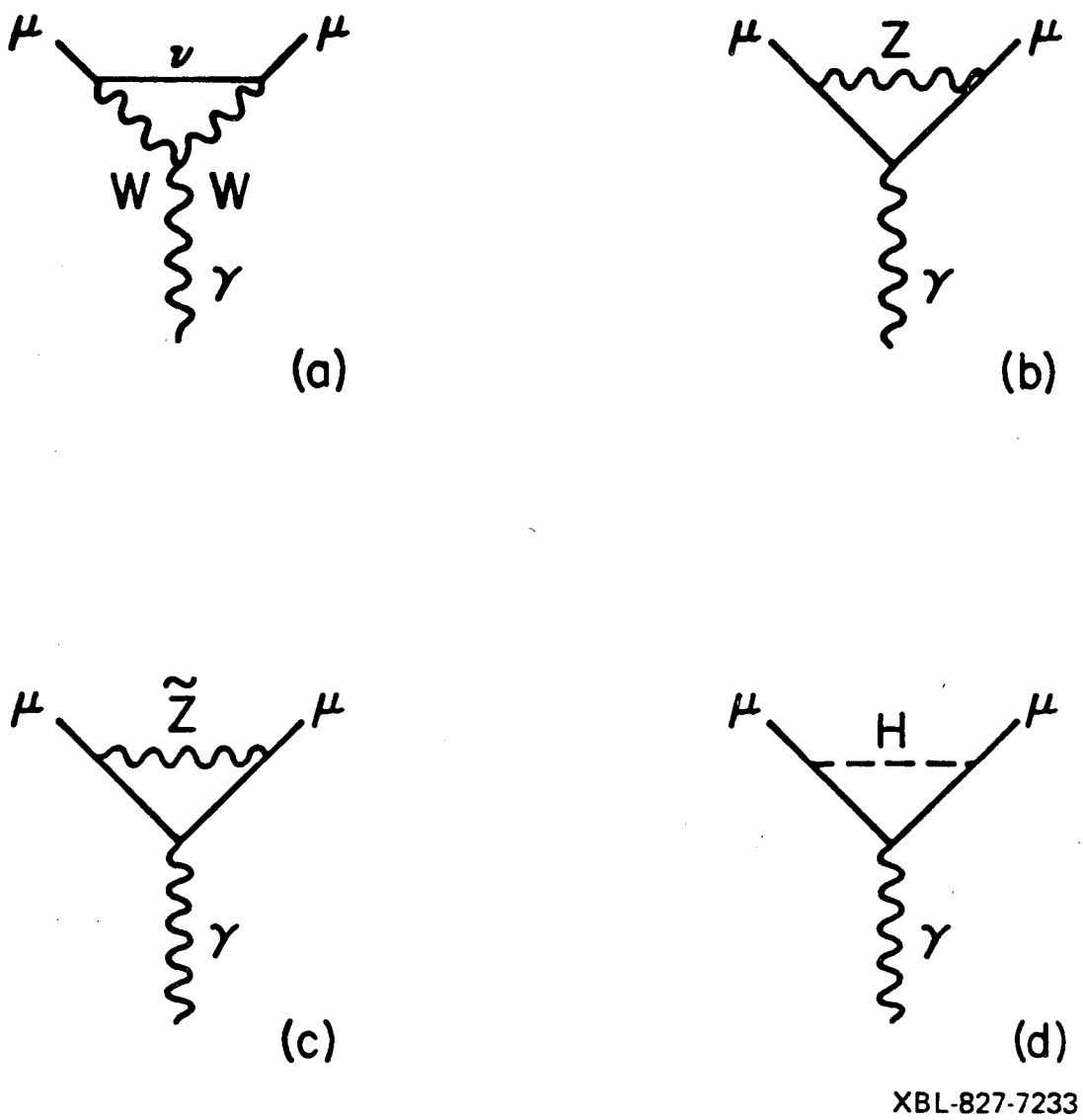

FIG. 7

II. MASS EVOLUTION IN UNIFIED THEORIES

INTRODUCTION

Grand unified theories (GUTs) [1], based originally on speculation about a symmetry group relating low-energy particle interactions of apparently different strengths, now enjoy much respect among theorists thanks partly to some phenomenological success. Three major predictions are usually regarded as characteristic of a broad class of grand unified models [2]:

(1) The finite lifetime of nucleons.

(2) The value of $\sin^2\theta$ at low energy renormalized from its value at the grand unification mass (GUM) scale.

(3) Certain fermion mass ratios at low energy renormalized down from their GUM values.

Unless prohibited explicitly by some kind of discrete symmetry, the decay of nucleons is inherent in most grand unified models, because of the presence of gauge bosons which carry quantum numbers of both quarks and leptons. Most theoretical estimates of the proton lifetime [3] border on the current experimental lower limit ($\tau_{p,\,exp} > 1 \sim 2 \cdot 10^{30}$ yr) [4]. A spectacular confirmation of this prediction may soon come from the search for proton decay currently under way [5]. Predictions (2) and (3) are also direct consequences of a basic concept GUTs are founded on; coupling constants are functions of the energy scale and evolve according to the appropriate renormalization group equations. In the minimal SU(5) model, for example, where $\sin^2\theta = \frac{3}{8}$ and $\frac{M_b}{M_\tau} = 1$ at GUM, low energy

values for these parameters have been shown to be consistent with data ($\sin^2\theta \simeq .206 \sim .216$ [6], $\frac{M_b}{M_\tau} \sim 3$ [7,8]).

The evolution of $\sin^2\theta$ is governed by the β functions for the coupling constants. The evolution of mass is usually treated in the same manner; mass is considered as another parameter receiving multiplicative renormalization. Thus the scale dependence of mass involves the anomalous dimension of the mass operator which is calculated perturbatively. However, there has been some discrepancy in the literature regarding gauge invariance of this procedure. It is the purpose of this chapter to clarify some of that confusion by recalling that in unified theories tree level fermion masses arise from Yukawa couplings. It is shown that the formula for mass evolution is not only gauge invariant but also has a very simple expression in the sense that it only depends on the representation content of the fermions and not on that of Higgs.

The organization of this chapter is as follows. Section 1 reviews the concept of mass evolution and the previous treatment of mass ratios in GUTs. In Section 2, a chiral U(1) model is considered, and the explicitly gauge invariant expression for the running mass is derived to the one loop level. In Section 3, the result of Section 2 is generalized to a non-Abelian case. The expression for the anomalous mass dimension is shown to be Higgs-independent as well as gauge invariant. In Section 4, a further extension is made to include the effect of supersymmetric partners of ordinary particles in the loop. Section 5 contains some applications of the formulas derived in the previous sections.

1. REVIEW OF THE PREVIOUS TREATMENT OF MASS EVOLUTION IN GUTs

A basic idea of grand unified theories is that various coupling constants associated with low-energy gauge groups evolve at different rates to merge into a single parameter at some large mass scale (GUM) [9]. The dependence of a coupling constant g_i on the scale (μ) is given by:

$$\frac{dg_i}{d\ln\mu} = \beta_i(g_i) \ , \tag{1}$$

where β_i are calculable to a given order in perturbation theory from the renormalization of a three-point gauge vector vertex function [10]. Thus $\sin^2\theta$, or its equivalent, which is essentially the ratio of two coupling constants subject to different renormalization group equations, is renormalized at low energy to a value different from its GUM value which is determined simply by the structure of the unifying group.

The mass of a fermion m, if treated as a coupling constant receiving multiplicative renormalization, evolves according to the following equation [7]:

$$\frac{dm}{d\ln\mu} = \gamma_m m \ , \tag{2}$$

where γ_m is the anomalous mass dimension, which is calculable from the renormalization of a two-point mass insertion operator.

To lowest order, β_i and γ_m are written as:

$$\beta_i = -\beta_i^0 g_i^3 \tag{3a}$$

$$\gamma_m = -\sum_i \gamma_{m_i}^0 g_i^2 . \tag{3b}$$

From eqs. (1), (2), (3a,b), the ratio of the fermion masses at two different scales is:

$$\frac{m(\mu_1)}{m(\mu_2)} = \prod_i \left(\frac{g_i^2(\mu_1)}{g_i^2(\mu_2)} \right)^{\frac{\gamma_{m_i}^0}{2\beta_i^0}} \tag{4}$$

β_i^0 is well known [11]:

$$\beta_i^0 = \frac{1}{16\pi^2} \left[\frac{11}{3} \mathcal{C}_A - \frac{4}{3} \mathcal{T}_F \right] , \tag{5}$$

Where $\mathcal{C}_A$ is the quadratic Casimir invariant for the adjoint representation of the gauge group, and $\mathcal{T}_F$ is defined in

$$\mathrm{tr}\ (T_F^a T_F^b) = \mathcal{T}_F \delta^{ab} , \tag{6}$$

T_F^a being a matrix representation for fermions. The first computation of γ_m^0 for an arbitrary gauge group was done by Nanopoulos and G. G. Ross [12], who considered the diagram (a) in Fig. 1 in the Landau gauge (where the gauge parameter $\alpha = 0$). Although, in general, all three diagrams in Fig. 1 contribute to γ_m^0, in the Landau gauge the fermion wave function renormalization is absent, and the answer they obtained is gauge invariant:

$$\gamma_m^0 = \frac{3}{8\pi^2} \, \phi_F \, , \tag{7}$$

where ϕ_F is the quadratic Casimir invariant for the fermion representation.

Now we briefly discuss the lepton-quark mass ratios in SU(5) [13]. If a single Higgs transforming as a $\underset{\sim}{5}$ under SU(5) gives mass to fermions through Yukawa terms, $m_D = m_E$ holds at GUM, where D and E denote a charge $-\frac{1}{3}$ quark and a charged lepton, respectively. As we go down in energy, D and E evolve differently in mass, since they have different SU(3) X SU(2) X U(1) quantum numbers. From eq. (4),

$$\frac{m_D(\mu)}{m_E(\mu)} = \prod_i \left(\frac{g_i^2(\mu)}{g_i^2(GUM)} \right)^{\frac{\Delta\gamma_{m_i}^0}{2\beta_i^0}} \, , \tag{8}$$

where $\Delta\gamma_{m_i}^0$ is the difference between $\gamma_{m_i}^0$'s for D and E, and i refers to SU(3), $SU(2)_L$, or U(1). The SU(3) corrections are dominant in eq. (8), and Chanowitz et. al. [7] applied eq. (8) for SU(3) to obtain $\frac{m_D}{m_E} \simeq 3$ at low energy, which works well for the third generation. This lowest order result cannot be directly applied to the first or second generation, because at momenta of the order of m_d or m_s, α_s is not small [14].

Although $SU(2)_L$ X U(1) corrections in eq. (8) are only about 10% of SU(3) corrections, some confusion arose in the literature when γ_m^0 for $SU(2)_L$ X U(1) computed in two different gauges gave different answers [7,15]. This apparent non-gauge invariance of γ_m for chiral theories is in fact not surprising, since the gauge dependence in the contribution from three diagrams in Fig. 1 is not

cancelled when left- and right-handed fermions have different wave function renormalizations. For example, in the case of $SU(2)_L$ the diagrams 1(a) and 1(c) give zero since the right-handed fermions do not couple to SU(2) bosons, and the only remaining diagram (1(b)) contributes a gauge dependent wave function renormalization.

This was also pointed out explicitly by Elias [16] who used the simple example of a chiral U(1) model, in which left- and right-handed fermions have charges a_L and a_R, with $a_L \neq a_R$ in general. The mass renormalization was done on a massive fermion propagator to yield, to one loop order,

$$\gamma_m = \frac{g^2}{16\pi^2} \left[- (6 + 2\alpha)\ a_L\ a_R + \alpha\ (a_L^{\ 2} + a_R^{\ 2}) \right] , \qquad (9)$$

where α is the gauge parameter in the vector propagator:

$$- i\ \frac{g^{\mu\nu} - (1 - \alpha)\ \frac{k^\mu k^\nu}{k^2}}{k^2} .$$

Eq. (9) is identical to the sum of the contributions from the three diagrams in Fig. 1. His point, illustrated further with specific examples from GUTs, was that in chiral theories although the anomalous dimensions of individual mass operators are in general gauge dependent, the ratios of masses evolve in a gauge-independent way.

However, Georgi and Nanopoulos [17] noted that the proper procedure is to consider the Higgs-fermion-fermion vertex which serves to give mass to fermions at the tree level in unified theories. Since a Yukawa term $h\ \bar{\Psi}_L \phi \Psi_R$ is gauge invariant, its anomalous

dimension is expected to be also gauge invariant at least to the one loop order [11], while the mass insertion operator $m\bar{\psi}\psi$ is not gauge invariant in chiral theories. The evolution of mass, at least in the intermediate energy range (between the SU(5) and SU(2) X U(1) breaking scales), is essentially governed by the scale dependence of the Yukawa coupling h:

$$\frac{dh}{d\ln\mu} = \gamma_h h \,. \tag{10}$$

To lowest order,

$$\gamma_h = - \Sigma \gamma_{h_i}^{0} g_i^2 \tag{11}$$

If a single Higgs is used in all the Yukawa terms in question the ratio of fermion masses is given by that of the corresponding Yukawa couplings. In the next two sections, gauge invariance of this procedure is demonstrated for chiral abelian and non-abelian theories.

2. THE CHIRAL ABELIAN CASE

We use the notation (a_L, a_R) introduced in the previous section. The relevant diagrams contributing to γ_h are shown in Figs. 2(a) and 3. The renormalized Higgs-fermion-fermion coupling h_R in terms of the bare h_o is given by:

$$h_R = h_o \frac{(Z_L Z_R Z_H)^{\frac{1}{2}}}{Z_1 Z_2 Z_3} \,, \tag{1}$$

Where Z_L, Z_R, Z_H are wave function renormalization factors for the left-handed fermion (diagram 3(a)), the right-handed fermion (diagram 3(b)), and the Higgs (diagram 3(c)), and Z_1, Z_2, Z_3 are the renormalization factors for diagrams 3(d), 3(e), 3(f), respectively.

The contribution from each Z factor to γ_h can be read off from its logarithmically divergent term; the negative of the coefficient of the term proportional to $\ln \frac{\Lambda}{\mu}$ (when regularized with cutoff Λ) or $\frac{1}{4-n}$ (when dimensionally regularized) is weighted by an appropriate factor from eq. (1) ($\frac{1}{2}$ for Z_L, Z_R, Z_H, and -1 for Z_1, Z_2, Z_3). For example, from diagram 3(a), we have

$$Z_L = 1 - \frac{g^2}{8\pi^2} \frac{a_L^2}{4-n} \alpha \quad . \tag{2}$$

Thus its contribution to γ_h is:

$$\alpha \frac{g^2}{16\pi^2} a_L^2 \quad . \tag{3}$$

We now list the contributions to γ_h from each of the six diagrams in fig. 3:

$$\gamma_h^{(a)} = \alpha \frac{g^2}{16\pi^2} a_L^2 \tag{4a}$$

$$\gamma_h^{(b)} = \alpha \frac{g^2}{16\pi^2} a_R^2 \tag{4b}$$

$$\gamma_h^{(c)} = -(3+\alpha) \frac{g^2}{8\pi^2} a_L a_R \tag{4c}$$

$$\gamma_h^{(d)} = -\alpha \frac{g^2}{8\pi} a_L (a_L - a_R) \tag{4d}$$

$$\gamma_h^{(e)} = \alpha \frac{g^2}{8\pi^2} a_R (a_L - a_R) \tag{4e}$$

$$\gamma_h^{(f)} = -(3 - \alpha) \frac{g^2}{16\pi^2} (a_L - a_R)^2 \tag{4f}$$

Notice we have used the fact that the Higgs charge in diagrams 3 (d, e, f) is required to be $(a_L - a_R)$ from gauge invariance of the Yukawa term.

The sum of eqs. (4a) through (4f) gives

$$\gamma_h = -\frac{3}{16\pi^2} g^2 (a_L^2 + a_R^2) , \tag{5}$$

which is gauge invariant. If we compare eq. (5) with eq. (1.9), we see that Elias' result corresponds to dropping diagrams 3 (d, e, f), as mentioned before. It can be also seen at this point why the mass ratio is guaranteed to be invariant even in the previous formulation in which a mass insertion is renormalized. The evolution of the ratio of two masses M_1 and M_2 is essentially governed by the difference between their anomalous mass dimensions. In the chiral abelian case, from eq. (1.9),

$$\gamma_{M_1} - \gamma_{M_2} = \frac{g^2}{16\pi^2} \Big\{ -6 (a_L^{(1)} a_R^{(1)} + a_L^{(2)} a_R^{(2)}) + \alpha [(a_L^{(1)} - a_R^{(1)})^2 - (a_L^{(2)} - a_R^{(2)})^2] \Big\} . \tag{6}$$

In unified theories where fermion masses arise from Yukawa terms, the α - dependent term in eq. (6) is zero, since $(a_L - a_R)$ for any fermion is fixed to be equal to the charge of the Higgs in the Yukawa term. Stated differently, the reason the calculation of the ratio in Landau gauge turned out to be correct is that in that gauge only diagrams 3 (c) and 3 (f) are non-zero. The former is the only one calculated by Buras et al. [8], and the latter, being only dependent on Higgs, cancels in the mass ratio.

3. THE NON-ABELIAN CASE

We generalize in this section the calculation of the previous section to a non-abelian case. The Yukawa terms are written as:

$$C_{ijk}\ \bar{\psi}_L^{\,i}\ \psi_R^{\,j}\ \phi^k\ . \tag{1}$$

(See Fig. 2(b)).

Analogously to the requirement in the abelian case that the Higgs charge be fixed to $(a_L - a_R)$, gauge invariance of the Yukawa terms implies [18] that

$$C_{ijm}\ (T_H^{\,a})_{\,mk} = (T_L^{\,a})_{\,ni}\ C_{njk} - C_{ilk}\ (T_R^{\,a})_{\,lj}, \tag{2}$$

where $T_H^{\,a}$, $T_L^{\,a}$, $T_R^{\,a}$ are the matrices for Higgs, left-handed, and right-handed fermion representations.

The same relation that was mentioned in the previous section between the Z factors and their contributions to γ_h is used. It

turns out that these contributions are expressed solely in terms of the quadratic Casimir invariants for the Higgs, left-handed fermion, and right-handed fermion representations:

$$\not{C}_H \, \delta_{ik} = \sum_{a,j} (T_H^a)_{ij} (T_H^a)_{jk} \tag{3a}$$

$$\not{C}_L \, \delta_{ik} = \sum_{a,j} (T_L^a)_{ij} (T_L^a)_{jk} \tag{3b}$$

$$\not{C}_R \, \delta_{ik} = \sum_{a,j} (T_R^a)_{ij} (T_R^a)_{jk} \, . \tag{3c}$$

We now list the contributions to γ_h from each of the diagrams in Fig. 3. Diagrams 3 (a, b, f) give in a straight-forward way:

$$\gamma_h^{(a)} = \alpha \frac{g^2}{16\pi^2} \not{C}_L \tag{4a}$$

$$\gamma_h^{(b)} = \alpha \frac{g^2}{16\pi^2} \not{C}_R \tag{4b}$$

$$\gamma_h^{(f)} = -(3 - \alpha) \frac{g^2}{16\pi^2} \not{C}_H \, . \tag{4c}$$

Using the relation (1) to eliminate T_H^a in terms of T_L^a and T_R^a, we get from diagram 3 (c),

$$\gamma_h^{(c)} = (3 + \alpha) \frac{g^2}{16\pi^2} (\not{C}_H - \not{C}_L - \not{C}_R) \, . \tag{5}$$

Similarly, with eq. (1), diagrams 3 (d) and 3 (e) combine to give:

$$\gamma_h^{(d)+(e)} = -\alpha \frac{g^2}{8\pi^2} \not{\phi}_H \tag{6}$$

Putting eqs. (4), (5), (6) together, we have the final result:

$$\gamma_h = -\frac{3}{16\pi^2} g^2 (\not{\phi}_L + \not{\phi}_R). \tag{7}$$

Again eq. (7) is gauge invariant, and the dependence on the Higgs representation has also dropped out. This means that although the tree level mass relation certainly depends on which Higgs fields are used in the Yukawa terms, its subsequent evolution depends only on the representation content of fermions. Some applications of this simple formula will be made in Section 5.

4. INCLUSION OF SUPERSYMMETRIC PARTICLES

In this section we compute γ_h for supersymmetric theories. We only have to add to γ_h obtained in Section 3 the contributions from extra diagrams in which fermions, Higgs, and gauge bosons in the loop are replaced by their supersymmetric partners, denoted by ϕ_F, Ψ_H, and χ, respectively. Five such diagrams are shown in Fig. 4. They correspond to diagrams 3(a, b, d, e, f) in the previous section.

Contributions from diagrams 4(a, b, c, d, e) to γ_h are:

$$\gamma_h^{(a)} = \frac{g^2}{16\pi^2} \not{\phi}_L \tag{1a}$$

$$\gamma_h^{(b)} = \frac{g^2}{16\pi^2} \not{\phi}_R \tag{1b}$$

$$\gamma_h^{(c)} + \gamma_h^{(d)} = -\frac{g^2}{4\pi^2}\,\phi_H \tag{1c}$$

$$\gamma_h^{(e)} = \frac{g^2}{12\pi^2}\,\phi_H\,. \tag{1d}$$

Adding eqs. (1a) through (1d), we obtain the total contribution from supersymmetric partners to γ_h:

$$\gamma_h^{sup} = \frac{g^2}{48\pi^2}\,[-8\,\phi_H + 3\,(\phi_L + \phi_R)]\,. \tag{2}$$

Combining eq. (2) and eq. (3.7) from the previous section, we get the final result for γ_h in supersymmetric theories:

$$\gamma_h = -\frac{g^2}{24\pi^2}\,[4\,\phi_H + 3\,(\phi_L + \phi_R)]\,. \tag{3}$$

Some application of this formula will be considered in the next section.

5. APPLICATIONS

In this section we apply the formulas for mass evolution derived in the previous sections to certain GUTs. First we apply the formula for γ_h (eq. 3.7) to SU(5). We only need to compute the appropriate Casimirs for fermion representations. A useful relation is:

$$\phi_F = \frac{N}{\mathscr{D}}\mathscr{T}_F\,, \tag{1}$$

where N is the number of generators of the group, $\mathscr{D}$ the dimension of

the fermion representation matrix T_F^a, and $\mathcal{T}_F$ was defined in eq. (1.6) of Section 1. For a fundamental representation of SU(N), $\mathcal{T}_F = \frac{1}{2}$.

For $SU(3)_{color}$,

$$\phi_L = \phi_R = \frac{4}{3}, \tag{2}$$

which gives

$$\gamma_h = -\frac{1}{2\pi^2} g^2 . \tag{3}$$

From the β function for SU(3) (eq. 1.5), we have, for quarks,

$$\frac{m_q(\mu)}{m_q(GUM)} = \left(\frac{g_3^2(\mu)}{g_3^2(GUM)}\right)^{\frac{12}{33-2f}}, \tag{4}$$

where f is the number of quark flavors. This agrees with the result given in ref. 7.

Similarly, for $SU(2)_L$ we have

$$\phi_L = \frac{3}{4} \tag{5a}$$

$$\phi_R = 0 \tag{5b}$$

$$\gamma_h = -\frac{9}{64\pi^2} g_2^2 \tag{5c}$$

$$\beta = -\frac{(11-f)}{24\pi^2} g_2^3 \tag{5d}$$

Thus the $SU(2)_L$ contribution to the mass ratio is:

$$\frac{m\ (\mu)}{m\ (GUM)} = \left(\frac{g_2^{\ 2}\ (\mu)}{g_2^{\ 2}\ (GUM)} \right)^{\frac{27}{16(11 - f)}} \tag{6}$$

For U(1), we have

$$\phi_L = \frac{3}{5}\ a_L^{\ 2} \tag{7a}$$

$$\phi_R = \frac{3}{5}\ a_R^{\ 2} \tag{7b}$$

$$\gamma_h = -\frac{9\ g^2}{80\pi^2}\ (a_L^{\ 2} + a_R^{\ 2}) \tag{7c}$$

$$\beta = \frac{f}{24\pi^2}\ g^3\ . \tag{7d}$$

The U(1) contribution to the mass ratio thus becomes:

$$\frac{m\ (\mu)}{m\ (GUM)} = \left(\frac{g^2\ (\mu)}{g^2\ (GUM)} \right)^{-\frac{27}{20f}\ (a_L^{\ 2} + a_R^{\ 2})}\ . \tag{8}$$

For ν, e, u, and d, $a_L^{\ 2} + a_R^{\ 2}$ equals $\frac{1}{4}$, $\frac{5}{4}$, $\frac{17}{36}$, and $\frac{5}{36}$, respectively.

Now we apply the formula for γ_h (eq. 4.3) to supersymmetric SU(5). Considering only the dominant SU(3) corrections, we have

$$\gamma_h = -\frac{g_3^{\ 2}}{3\pi^2}\ , \tag{9}$$

where we have used eq. (2) and $\phi_H = 0$.

The β function for supersymmetric theories is given by [19]:

$$\beta_i = -\frac{1}{16\pi^2}(3\,\mathcal{C}_A - 2\mathcal{T}_F)\,g_i^{\,3}\,. \tag{10}$$

Thus for quarks the mass ratio becomes:

$$\frac{m\,(\mu)}{m\,(\mathrm{GUM})} = \left(\frac{g_3^{\,2}\,(\mu)}{g_3^{\,2}\,(\mathrm{GUM})}\right)^{\frac{8}{3}\,\frac{1}{(9-f)}}\,. \tag{11}$$

We note from eqs. (3) and (9) that for SU(3) the anomalous mass dimension for supersymmetric theories is smaller in magnitude than for ordinary theories. However, it is interesting that for three generations of fermions the gauge couplings evolve at slower rates in supersymmetric theories than in ordinary theories (see eqs. (10) and (1.5)) for SU(3) [19], which nearly compensates the change in γ_h [20]. For the third generation (with f = 6), eq. (11) gives

$$\frac{m_b}{m_\tau} \cong 2.8\,.$$

Thus the successful prediction in the minimal SU(5) model for $\frac{m_b}{m_\tau}$ is essentially preserved in a supersymmetric extension.

We can apply our results to models in which there is evolution above SU(5). For example, in a model by Elias [21], the unifying group SO(10) breaks down to SU(5) at M_5, and all fermion masses are assumed equal at GUM. As we go down from GUM to M_5, particles belonging to different representations of SU(5) split in mass. The

evolution of mass ratios is governed by the Casimirs for SU(5):

$$\phi\,(\underset{\sim}{5}) = \frac{12}{5} \tag{12}$$

$$\phi\,(\underset{\sim\sim}{10}) = \frac{18}{5}\,. \tag{13}$$

From eq. (1.4), we have

$$\ln \frac{r_E}{r_N} = \phi\,(5) + \phi\,(10) - \phi\,(5) = \frac{18}{5} \tag{14a}$$

$$\ln \frac{r_U}{r_D} = \phi\,(10) + \phi\,(10) - \phi\,(5) - \phi\,(10) = \frac{6}{5}\,, \tag{14b}$$

where $r_E = \dfrac{m_E\,(M_5)}{m_E\,(\mathrm{GUM})}$, etc., and E, N, U, D denote a charged lepton, a neutrino, a charge $\frac{2}{3}$ quark, and a charge $-\frac{1}{3}$ quark. From eqs. (14 a,b), we obtain

$$\left.\frac{m_E}{m_N}\left(\frac{m_D}{m_U}\right)^3\right|_{\text{at low energy}} \cong \left.\frac{m_E}{m_N}\left(\frac{m_D}{m_U}\right)^3\right|_{\text{at } M_5} = 1\,. \tag{15}$$

For second and third generations, this implies

$$m_{\nu_\mu} \simeq 35\ \text{eV} \tag{16a}$$

$$m_{\nu_\tau} \simeq 1.8\ \text{MeV (with } m_t = 50\ \text{GeV})\,. \tag{16b}$$

FIGURE CAPTIONS

Fig. 1 Diagrams contributing to the renormalization of a mass insertion operator represented by the cross.

Fig. 2 The Higgs-fermion-fermion vertex (a) in a chiral abelian theory, and (b) in non-abelian theories.

Fig. 3 Diagrams contributing to the renormalization of a Yukawa coupling.

Fig. 4 Additional diagrams contributing to the anomalous mass dimension in supersymmetric theories. ϕ_F, χ, and Ψ_H are supersymmetric partners of fermions, gauge bosons, and Higgs, respectively.

REFERENCES

[1] H. Georgi and S. L. Glashow, Phys. Rev. Lett. 32, 438 (1974); J. C. Pati and A. Salam, Phys. Rev. Lett. 31, 661 (1973).

[2] For a review and references, see, for example, P. Langacker, Phys. Rep. 72 C, 185 (1981).

[3] V. S. Berezinski, B. L. Ioffe and Ya. I. Kogan, Phys. Lett. 105 B, 33 (1981) and references contained therein.

[4] J. Learned, F. Reines and A. Soni, Phys. Rev. Lett. 43, 907 (1979); E. N. Alekseev et al., report, XVIIth Intern. Cosmic Ray Conf. (1981).

[5] S. Miyake and V. S. Narasimham; R. I. Steinberg; M. A. Shupe; E. Fiorini; R. Barloutaud; C. Wilson; D. Sinclair and T. W. Jones, in The Second Workshop on Grand Unification, ed. J. Leveille, L. Sulak and D. Unger (Birkhauser, Boston, 1981).

[6] W. J. Marciano and A. Sirlin, in The Second Workshop on Grand Unification (see ref. 4).

[7] M. S. Chanowitz, J. Ellis, and M. K. Gaillard, Nucl. Phys. B 128, 506 (1977).

[8] A. J. Buras et al., Nucl. Phys. B 135, 66 (1978).

[9] H. Georgi, H. R. Quinn and S. Weinberg, Phys. Rev. Lett. 33, 451 (1974).

[10] H. D. Politzer, Phys. Rep. 14 C, 129 (1974).

[11] D. J. Gross and F. Wilczek, Phys. Rev. D 8, 3622 (1973).

[12] D. V. Nanopoulos and G. G. Ross, Phys. Lett. B 56, 279 (1975).

[13] H. Georgi and S. L. Glashow, ref. 1.

[14] H. Georgi and C. Jarlskog, Phys. Lett. 86 B, 297 (1979).

[15] D. V. Nanopoulos and D. A. Ross, Nucl. Phys. B 157, 273 (1979).

[16] V. Elias, Phys. Rev. D 21, 1113 (1980).

[17] H. Georgi and D. V. Nanopoulos, Phys. Lett. 82 B, 329 (1979).

[18] T. P. Cheng, E. Eichten and L. F. Li, Phys. Rev. D 9, 2259 (1974).

[19] S. Dimopoulos, S. Raby, F. Wilczek, Phys. Rev. D 24, 1681 (1981).

[20] J. Ellis, D. V. Nanopoulos and S. Rudaz, CERN-TH3199 (1981); M. B. Einhorn and D. R. T. Jones, Nucl. Phys. B 196, 475 (1982); L. E. Ibanez and G. G. Ross, Oxford-TP-65-81.

[21] V. Elias, Univ. of Toronto preprint (Jan. 1980).

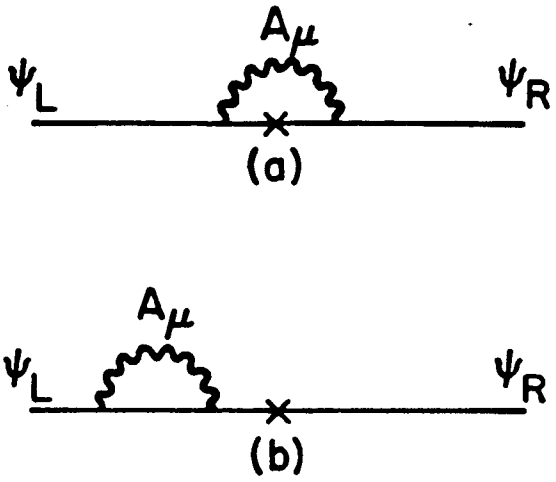

FIG. 1

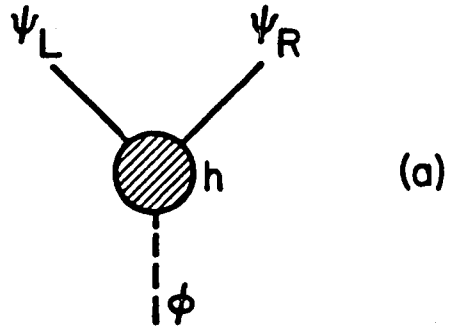

FIG. 2

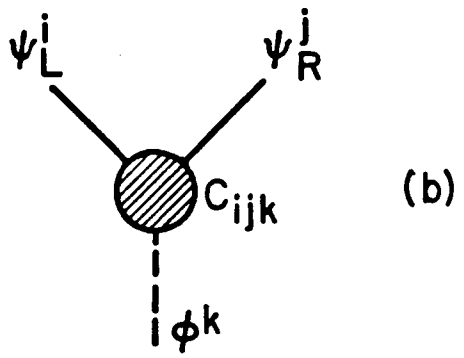

XBL-827-7230

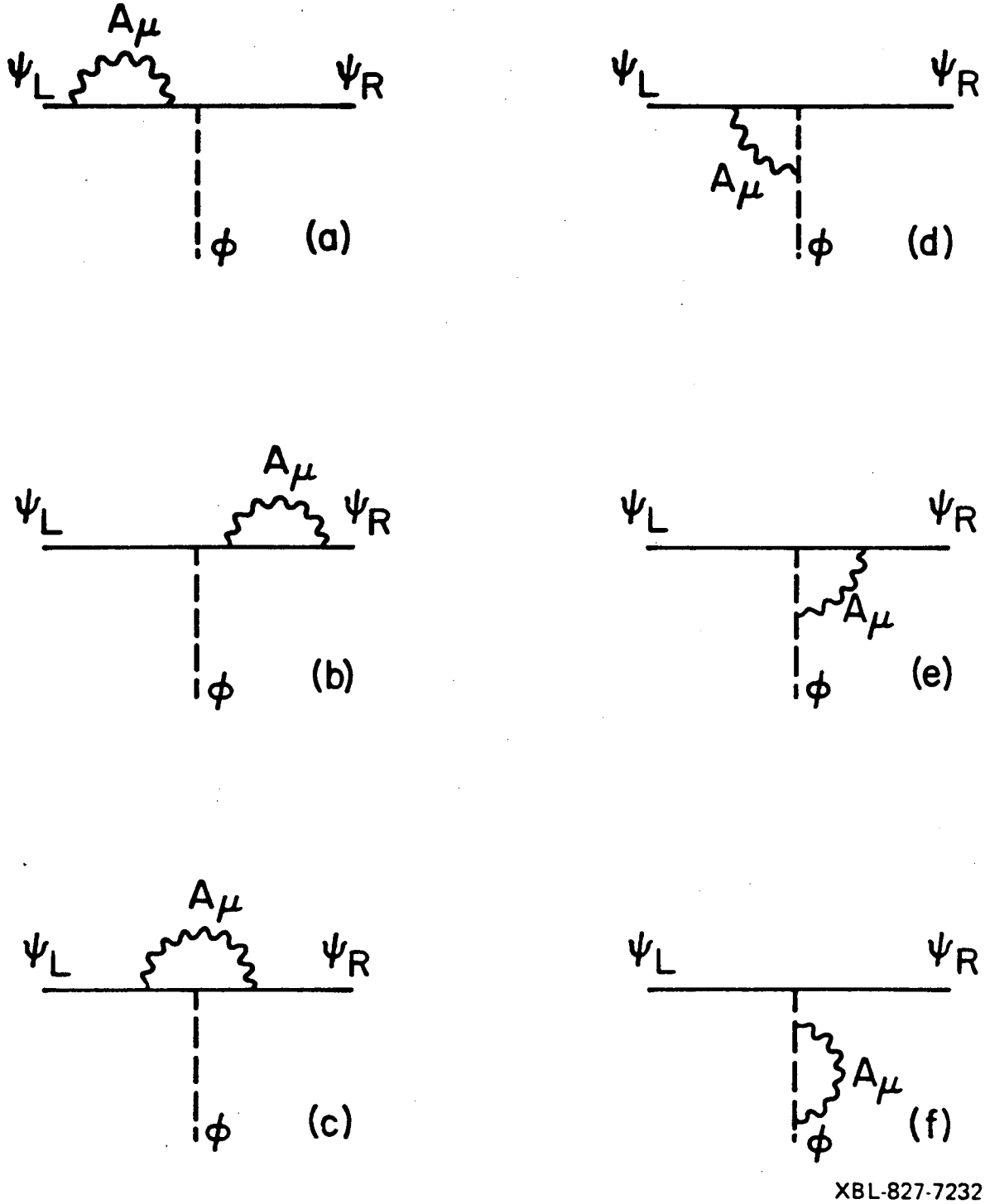
A_μ
ψ_L
ψ_R
ϕ
(a)
ψ_L
ψ_R
A_μ
ϕ
(d)
A_μ
ψ_L
ψ_R
ϕ
(b)
ψ_L
ψ_R
A_μ
ϕ
(e)
A_μ
ψ_L
ψ_R
ϕ
(c)
ψ_L
ψ_R
A_μ
ϕ
(f)
XBL-827-7232

FIG. 3

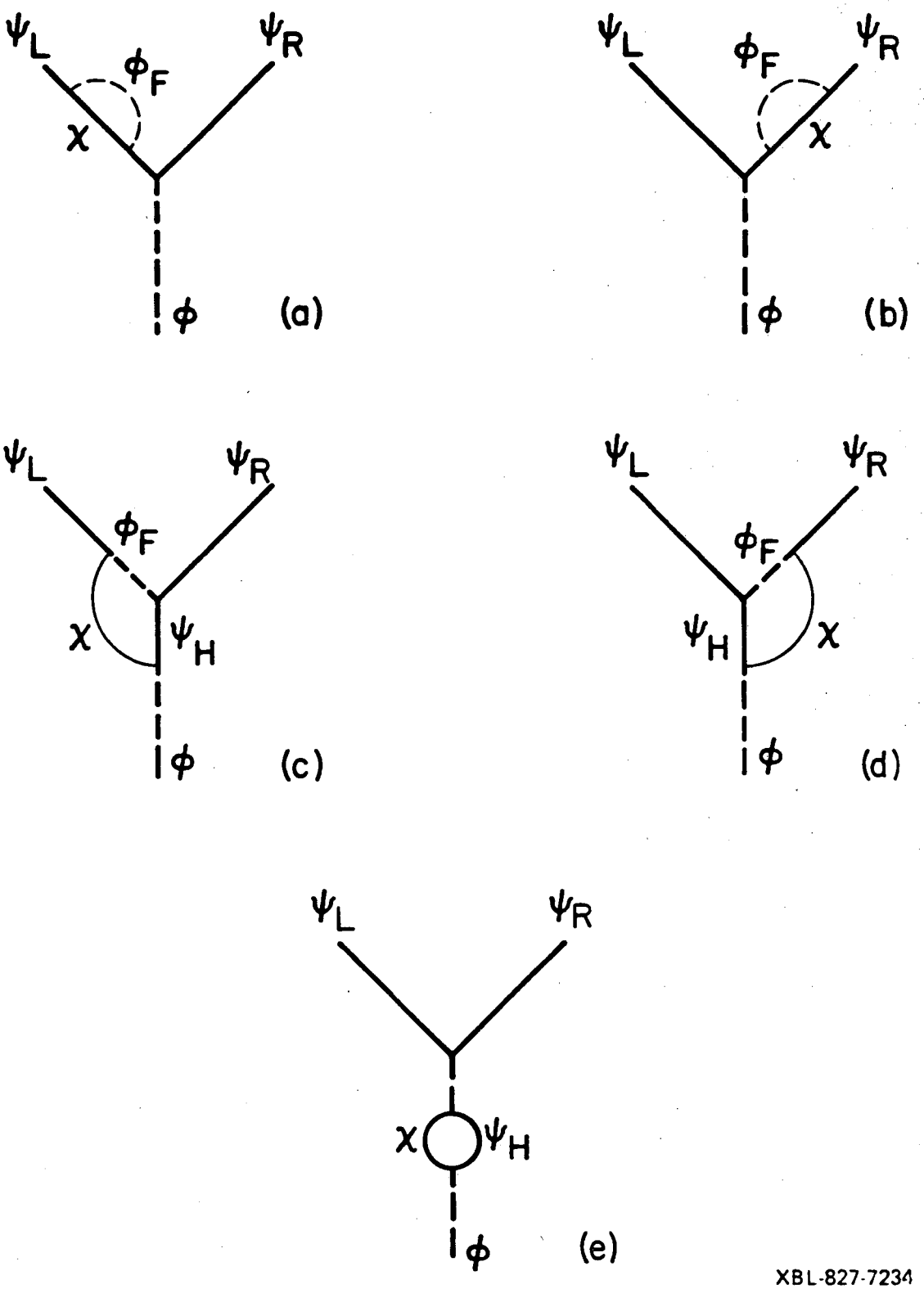

XBL-827-7234

FIG. 4

III. HEAVY LEPTON POLARIZATION AT Z PEAK

INTRODUCTION

While all low-energy data point to the existence of a massive neutral gauge boson, its direct production remains as the definitive test of the standard electroweak model [1]. If the Z is indeed discovered in the next generation of colliding beam experiments, its mass and width will provide information on $\sin^2\theta$ and the number of different species of neutrinos, among other things. In addition, experiments near the Z peak will probe into the nature of the fermion couplings to Z. In this chapter we consider one such experiment, namely, the measurement of the polarization of a heavy lepton produced in pairs in e^+e^- annihilation. This process is of particular interest, since it is the only one sensitive to the relative sign between the vector and axial $Z\bar{f}f$ couplings in the absence of polarized beams. Furthermore, it benefits greatly from the high event rate at the Z peak, while at low energy such an experiment is probably not feasible. In constrast, the forward-backward asymmetry in lepton pair production, which is another high-priority experiment at the Z peak, measures only the magnitude of the axial couplings, and some low-energy data are already available [2].

The first treatment by Tsai [3] of heavy lepton pair production in e^+e^- annihilation and their subsequent decays focused on the production of τ pairs slightly above the threshold, where the photon exchange is dominant. The full formula for the cross-section for lepton pair production including the photon and the weak boson exchanges

was derived by Budny [4], from which the longitudinal polarization of a lepton is immediately obtained. The extraction of the polarization of a heavy lepton L from its decay products at the Z peak was discussed by Goggi [5] and Augustin [6] in the context of LEP, who considered the decays $L \to e \nu\nu$ and $L \to \pi \nu$, respectively. The purpose of this chapter is to extend their work in two aspects. First, we derive formulas involved in the production and the subsequent decays of heavy leptons of arbitrary mass. This analysis may be relevant for any possible sequential heavy lepton of mass $\lesssim \frac{M_z}{2}$. Secondly, the correlation between the spins of a heavy lepton pair is considered in the form of a cross-section for the production and the coincident decays of the pair.

The organization of this chapter is as follows. In Section 1, the full formula for the longitudinal polarization of a heavy lepton of arbitrary mass at arbitrary e^+e^- center of mass energy is derived. In Section 2, the purely leptonic decay of a heavy lepton of arbitrary mass is discussed. In Section 3, the decay in flight $L \to \pi \nu$ for arbitrary M_L is considered. In Section 4 the results of the previous sections are combined to give the final formula for heavy lepton decays in coincidence.

1. THE LONGITUDINAL POLARIZATION OF A HEAVY LEPTON

The average longitudinal polarization P_L of a lepton L produced in pairs is given by:

$$\langle P_L \rangle = \frac{\sigma_+ - \sigma_-}{\sigma_+ + \sigma_-} \quad . \tag{1}$$

$\sigma^{\pm}$ denote the production cross-sections for L with helicity ± 1, in which the helicity of the other lepton is summed over. If left- and right-handed fermions couple differently to the exchanged gauge boson, $\langle P_L \rangle$ is in general non-zero. Moreover, $\langle P_L \rangle$ has a linear dependence on g_v and g_A; $\langle P_L \rangle \sim g_v g_A$, which allows us to determine the relative sign of the vector and axial couplings.

To calculate $\langle P_L \rangle$ we need the spin-dependent cross-section σ for the process $e^+e^- \to \gamma^*, Z \to L^+L^-$. Generalizing the notation of Tsai [3], we write the cross-section as follows:

$$\frac{d\sigma}{d\Omega} \propto C_o + \vec{C}_1 \cdot \vec{S} + \vec{C}_2 \cdot \vec{S}' + \vec{S} \cdot \overleftrightarrow{C}_3 \cdot \vec{S}' \quad , \tag{2}$$

where $\vec{S}$ and $\vec{S}'$ are the spins of L^- and L^+ in their rest frames. The diagrams contributing to this cross-section are shown in Fig. 1. If the axial part of the $Z\bar{L}L$ coupling is non-zero (as in the standard model) $\vec{C}_1$ and $\vec{C}_2$ are also expected to be non-zero. In Tsai's formula derived for low-energy e^+e^- annihilation where only the photon exchange was considered, the linear terms in the spins are absent, and $\langle P_L \rangle = 0$.

The angular distribution obtained from diagrams 1 (a,b) in terms of $\vec{S}$ and $\vec{S}'$, averaged over e^+e^- spins, is written as:

$$\frac{d\sigma}{d\Omega} = \frac{1}{(4\pi)^2} \frac{\beta}{s} \left\{ e^4 \, I_\gamma + 2 \, e^2 \, \frac{s}{s - M_z^2} \, I_{int} + \left[\frac{s}{s - M_z^2} \right]^2 I_z \right\}, \tag{3}$$

where β is the velocity of $L^{\pm}$ and s the total energy squared in the

center of mass system. The three terms in eq. (3) represent contributions from the photon exchange, the γ - Z interference, and the Z exchange, respectively. I_γ, I_{int}, and I_z contain constant, linear, and bilinear terms in the heavy lepton spins. The coefficients of these terms for each of the I's are listed below, denoted by C_o, $\vec{C}_1$, $\vec{C}_2$, and $\overleftrightarrow{C}_3$ in accordance with eq. (2). (For the coordinate system used, including the definition of θ , refer to Fig. 2.)

For I_γ ,

$$C_o = 1 + \cos^2\theta + \frac{\sin^2\theta}{\gamma}$$

$$\vec{C}_1 = \vec{C}_2 = 0$$

$$\overleftrightarrow{C}_3 = \begin{array}{c} \\ x' \\ y' \\ z' \end{array} \begin{array}{c} \begin{array}{ccc} x & y & z \end{array} \\ \begin{bmatrix} (1 + \frac{1}{\gamma^2}) \sin^2\theta & 0 & \frac{1}{\gamma} \sin 2\theta \\ 0 & -\beta^2 \sin^2\theta & 0 \\ \frac{1}{\gamma} \sin 2\theta & 0 & 1 + \cos^2\theta - \frac{\sin^2\theta}{\gamma^2} \end{bmatrix} \end{array} , \tag{4}$$

where $\gamma = \frac{1}{\sqrt{1 - \beta^2}}$. This agrees with the result given by Tsai.

For I_{int} ,

$$C_o = g_v^{\,2} (1 + \frac{1}{\gamma^2}) + 2 \beta g_A^{\,2} \cos\theta + \beta^2 g_v^{\,2} \cos^2\theta$$

$$\vec{C}_1 = \vec{C}_2 \tag{5}$$

$$= [g_v g_A \frac{1}{\gamma} (2 + \beta \cos\theta) \sin\theta,\ 0,\ g_v g_A (\beta + 2\cos\theta + \beta \cos^2\theta)]$$

$$\overleftrightarrow{C}_3 = \begin{bmatrix} g_v^2 (1 + \frac{1}{\gamma^2}) \sin^2\theta & 0 & \frac{\sin\theta}{\gamma} (2g_v^2 \cos\theta + \beta g_A^2) \\ 0 & -\beta^2 g_v^2 \sin^2\theta & 0 \\ \frac{\sin\theta}{\gamma} (2g_v^2 \cos\theta + \beta g_A^2) & 0 & \beta^2 g_v^2 + 2\beta g_A^2 \cos\theta + (1 + \frac{1}{\gamma^2}) g_v^2 \cos^2\theta \end{bmatrix}.$$

For I_z,

$$C_o = (g_v^2 + g_A^2)^2 + \frac{1}{\gamma^2} (g_v^4 - g_A^4) + 8 g_v^2 g_A^2 \beta \cos\theta + (g_v^2 + g_A^2)^2 \beta^2 \cos^2\theta$$

$$C_{1x} = C_{2x} = 2 g_A g_v \frac{1}{\gamma} [2 g_v^2 + \beta (g_v^2 + g_A^2) \cos\theta] \sin\theta$$

$$C_{1y} = C_{2y} = 0$$

$$C_{1z} = C_{2z} = 2 g_v g_A [\beta (g_v^2 + g_A^2) + 2 (g_v^2 + \beta^2 g_A^2) \cos\theta + \beta (g_v^2 + g_A^2) \cos^2\theta]$$

$$C_{3xx} = [(g_v^4 - g_A^4) + \frac{1}{\gamma^2} (g_v^2 + g_A^2)^2] \sin^2\theta \tag{6}$$

$$C_{3yy'} = -(g_v^4 - g_A^4)\,\beta^2 \sin^2\theta$$

$$C_{3zz'} = \beta^2 (g_v^2 + g_A^2)^2 + 8\, g_v^2 g_A^2\, \beta \cos\theta + \left[(g_v^2 + g_A^2)^2 + \frac{g_v^4 - g_A^4}{\gamma^2}\right] \cos^2\theta$$

$$C_{3xz'} = C_{3zx'} = \frac{1}{\gamma}\left[4\,\beta\, g_v^2 g_A^2 \sin\theta + (g_v^4 + g_v^2 g_A^2) \sin 2\theta\right]$$

$$C_{3xy'} = C_{3yx'} = C_{3yz'} = C_{3zy'} = 0\ .$$

g_v and g_A in Eqs. (5) and (6) are the vector and the axial couplings of e (μ, τ) to Z:

$$\mathscr{L}_{int} = Z^\mu \bar{f} \gamma_\mu (g_v + g_A \gamma_5)\, f\ ,$$

where f = e, μ, or τ .

The coefficient of each spin term in $\frac{d\sigma}{d\Omega}(e^+e^- \to L^+L^-)$ can be read off from eqs. (3) through (6). For example, the $S_y S_y'$ term is given by:

$$-\frac{1}{(4\pi)^2}\frac{\beta^3}{s}\sin^2\theta \left\{ e^4 + 2e^2 \frac{s}{s - M_z^2} g_v^2 + \left[\frac{s}{s - M_z^2}\right]^2 (g_v^4 - g_A^4) \right\} S_y S_y' \qquad (7)$$

Note that the interchange of L^+ and L^- (charge conjugation) results in the sign flip of the linear terms in $\vec{S}$ and $\vec{S}'$. From the cross-section (eqs. (3) through (6)), $\langle P_L \rangle$ is obtained according to eq. (1).

We consider two special cases, near the Z peak.

(i) $\beta \to 0$ (near the threshold)

$$\frac{d\sigma}{d\Omega} = \frac{1}{2(4\pi)^2} \beta s \left[\frac{1}{s - M_z^2}\right]^2 g_v^2 \left\{ (g_v^2 + g_A^2) \left[1 + (\hat{k}\cdot\vec{S})(\hat{k}\cdot\vec{S}')\right] + 2 g_v g_A \left(\hat{k}\cdot\vec{S} + \hat{k}\cdot\vec{S}'\right) \right\} ,$$

where $\hat{k}$ is the unit vector in the direction of e^- (see Fig. 2.). Thus if $\xi = g_v g_A > 0$, both $\vec{S}$ and $\vec{S}'$ tend to be parallel to $\hat{k}$, and if $\xi < 0$ the two spins tend to be anti-parallel to $\hat{k}$.

(ii) $\beta \to 1$ (massless)

This is the case considered previously by other authors [5,6]. Summing over one lepton final state, and integrating over $\cos\theta$, we obtain the well known formula;

$$\langle P_L \rangle = \mp \frac{2\xi}{1 + \xi^2} \quad \text{for } L^{\pm} .$$

In discussing the correlation between the two lepton spins in Section 4, we use the cross-section itself which is folded with the decay spectra, rather than $\langle P_L \rangle$.

2. HELICITY ANALYSIS FROM $L \to \ell \nu \nu$

As the heavy lepton pair produced in e^+e^- annihilation decay in flight, their spin contents are transferred into the energy distribution of their decay products. Although the production cross-section of L^+L^- is reduced in the process by the branching ratios involved, the large cross-section near the Z peak compensates for this loss in rates to make this kind of analysis experimentally feasible. Two major decay modes have been studied. In this section we consider $L \to \ell \nu\nu$, where ℓ = e or μ. $L \to \pi\nu$ is presented in the next section. The leptonic decays have the advantage that they give a clean experimental signature in the form of μ e events. Even for a very heavy sequential lepton whose chain of decays may be more complicated, the formulas listed here may be relevant in the case of prompt decays into μ e.

The decay rate Γ for $L^- \to \ell^- \nu \bar{\nu}$ in the e^+e^- center of mass frame can be written as:

$$d\Gamma_\ell \propto (A + \vec{B} \cdot \vec{S})\, d^3\vec{q}\,, \qquad (1)$$

where $\vec{q}$ is the momentum of ℓ^-, and $\vec{S}$ the spin of L^- in its rest frame, as before. A and $\vec{B}$ are functions of $\vec{q}$, $\sqrt{s}$, and M_L. Since we are only interested in the energy spectrum, we can fix the momentum of L^- to be in the $\hat{Z}$ direction. We write, ignoring the mass of ℓ,

$$\frac{d\Gamma_\ell}{dx\ d\cos\theta} = \frac{G^2 M_L^5}{3 \cdot 2^6 \pi^3} \frac{1}{\gamma} [f(X, \cos\theta) + S_z\, g(X, \cos\theta)]\,, \qquad (2)$$

where $X = \frac{|\vec{q}|}{\frac{1+\beta}{4}\sqrt{s}}$ $(0 \leq X \leq 1)$, (3)

i.e. the normalized energy of ℓ, and θ is the polar angle for the beam axis (see Fig. 2).

f and g are given by:

$$f\ (X, \cos\theta) = \frac{(1+\beta)}{(1-\beta)^2}\ (1 - \beta\cos\theta)\ [3X^2 - 2X^3\ \frac{1-\beta\cos\theta}{1-\beta}] . \quad (4a)$$

$$g\ (X, \cos\theta) = \frac{(1+\beta)}{(1-\beta)^2}\ (\beta - \cos\theta)\ [2X^3\ \frac{1-\beta\cos\theta}{1-\beta} - X^2] . \quad (4b)$$

For $\beta = 0$, integrating eq. (2) over X, we recover the familiar angular distribution in the rest frame of L^- .

In obtaining the ℓ energy spectrum for arbitrary β, we note the kinematic constraint that the sum of neutrino four-mementa be time-like:

$$1 - \frac{X}{1-\beta}\ (1 - \beta\cos\theta) \geq 0 . \quad (5)$$

Thus the integration over θ differs in two regions of X:

$$-1 \leq \cos\theta \leq 1 \qquad \text{for} \quad 0 \leq X \leq \frac{1-\beta}{1+\beta} \quad (6a)$$

$$\frac{1}{\beta}\ (1 - \frac{1-\beta}{X}) \leq \cos\theta \leq 1 \qquad \text{for} \quad \frac{1-\beta}{1+\beta} \leq X \leq 1 . \quad (6b)$$

The resulting energy spectrum of ℓ^- is:

$$\frac{1}{\Gamma_\ell}\frac{d\Gamma_\ell}{dX} = F_\ell(X) + S_z\, G_\ell(X)\ , \tag{7}$$

where

$$F_\ell(X) = \begin{cases} \left[-\frac{4}{3}\frac{(3+\beta^2)}{1-\beta}X^3 + 6X^2\right]\ \frac{1+\beta}{(1-\beta)^2}, & 0 \le X \le \frac{1-\beta}{1+\beta} \\ \frac{1+\beta}{6\beta}\,(4X^3 - 9X^2 + 5)\ , & \frac{1-\beta}{1+\beta} \le X \le 1 \end{cases} \tag{8a}$$

$$G_\ell(X) = \begin{cases} \frac{\beta(1+\beta)}{3\,(1-\beta)^3}\,[16X^3 - 6\,(1-\beta)\,X^2]\ , & 0 \le X \le \frac{1-\beta}{1+\beta} \\ \frac{1+\beta}{6\beta^2}\,[2\,(3\beta+1)\,X^3 - 3\,(2\beta+1)\,X^2 + 1], & \frac{1-\beta}{1+\beta} \le X \le 1 \end{cases} \tag{8b}$$

Identifying S_z as the spin of L^- produced in e^+e^- collision, we replace it by $\langle P_L \rangle$ derived in the previous section. $F_\ell(X)$ and $G_\ell(X)$ are plotted in Fig. 3 for various values of β. For $\beta = 1$ eq. (7) reduces to the formula derived by Goggi [5,7]:

$$\frac{1}{\Gamma_\ell}\frac{d\Gamma_\ell}{dX} = \frac{1}{3}\,(4X^3 - 9X^2 + 5) + \frac{2\xi}{1+\xi^2}\,\frac{1}{3}\,(8X^3 - 9X^2 + 1)\ . \tag{9}$$

We mention in passing one quantity considered by Goggi which is sensitive to $\langle P_L \rangle$:

$$n = \frac{\int_{X_c}^{1} \left[\frac{d\Gamma}{dX}\right] dX}{\int_{0}^{X_c} \left[\frac{d\Gamma}{dX}\right] dX}\ , \tag{10}$$

where X_c is the zero of $G_\ell(X)$, as seen in Fig. 3(a). The denominator and the numerator of n change in the opposite direction from each other as $\langle P_L \rangle$ changes. For $\beta \neq 1$ there is more than one zero of $G_\ell(X)$ and an analogous quantity to n does not seem to be of much use. The spectrum $\frac{d\Gamma}{dX}$ for L^+, whose momentum lies in the $-\hat{Z}$ direction has the same form as eq. (7) with S_Z' replacing S_Z. Formulas (7) and (8) will be used in Section 4 to derive the cross-section for L^+L^- coincident decays.

3. HELICITY ANALYSIS FROM $L \to \pi \nu$

Another decay mode of L^- which can serve as a helicity analyzer is the process $L^- \to \pi^- \nu$. An advantage of this two-body decay is that the spin content of L^- decaying in flight is directly translated into the slope of the pion energy distribution. A disadvantage may be that for heavier leptons the hadronic decay channel may get complicated, which makes direct pion production difficult to analyze.

The formula for the pion angular distribution in the rest frame of L^- is well-known to be:

$$\frac{d\Gamma_\pi}{d\cos\theta} = \frac{f_\pi^2 G^2 M_L^3}{16\pi} (1 - R)^2 \frac{1}{2} (1 + S_Z \cos\theta) , \qquad (1)$$

where $R = \frac{M_\pi^2}{M_L^2}$.

In the center of mass frame the energy distribution is obtained easily from the boost along the $\hat{Z}$ direction;

$$\frac{d\Gamma_\pi}{dX} = \frac{f_\pi^2 G^2 M_L^3}{16\pi\gamma} (1 - R)^2 [F_\pi(X) + S_Z G_\pi(X)] , \qquad (2)$$

where X is the normalized pion energy, $\frac{2E_\pi}{\sqrt{s}}$, and

$$\frac{(1 + R) - \beta (1 - R)}{2} \leq X \leq \frac{(1 + R) + \beta (1 - R)}{2} . \qquad (3)$$

F_π and G_π are given by:

$$F_\pi(X) = \frac{1}{\beta(1 - R)} \qquad (4a)$$

$$G_\pi(X) = \frac{1}{\beta^2 (1 - R)} [2X - (1 + R)] . \qquad (4b)$$

The same expression as eq. (2) results for L^+ moving in the $-\hat{Z}$ direction with S_Z' replacing S_Z . Fig. 4 shows $\frac{1}{\Gamma_\pi} \frac{d\Gamma_\pi}{dX}$ for a representative value of $\langle P_L \rangle$ (with $\sin^2\theta = .2$), for various values of β.

4. CROSS-SECTION FOR COINCIDENT DECAYS

In the two previous sections we derived expressions for decay cross-sections in terms of the polarization of one heavy lepton with the helicity of the other summed over. From eqs. (1.3), (2.2), (3.2), we can get the cross-section σ_c for

$$e^+e^- \rightarrow \begin{cases} L^+ \rightarrow \ell^+ \nu\nu \text{ or } \pi^+ \nu \\ L^- \rightarrow \ell^- \nu\nu \text{ or } \pi^- \nu \end{cases} . \qquad (1)$$

σ_c contains information on the correlation between the two heavy lepton spins, and is given by

$$\sigma_c = \sigma (e^+e^- \to L^+L^-) B_i B_j , \tag{2}$$

where $B_{i,j}$ are the appropriate branching ratios (i, j = ℓ or π).

Since in deriving eqs. (2.2), (3.2) we chose $L^{\pm}$ momenta to be in $\mp \hat{Z}$ direction, the relevant part of eq. (1.3) can be written as:

$$\frac{d\sigma}{d\Omega} = a_1 + a_2 (S_Z + S_Z') + a_3 S_Z S_Z' , \tag{3}$$

where a_1, a_2, a_3 are functions of θ alone and can be read off from eqs. (1.3) through (1.6).

From eqs. (1.3), (2.2), (3.2), summing over S_Z and S_Z' we obtain

$$\begin{aligned} \frac{1}{\sigma_c} \frac{d\sigma_c}{dX_1\, dX_2} &= F_i (X_1) F_j (X_2) \\ &+ \frac{\int a_2\, d\Omega}{\int a_1\, d\Omega} [G_i (X_1) F_j (X_2) + F_i (X_1) G_j (X_2)] \\ &+ \frac{\int a_3\, d\Omega}{\int a_1\, d\Omega} G_i (X_1) G_j (X_2) , \end{aligned} \tag{4}$$

where X_1 and X_2 are normalized energies of ℓ or π (eqs. (2.3), (3.3)), and i, j can be either ℓ or π (eqs. (2.8), (3.4)).

The coefficients of the second and the third terms in eq. (4) are given by, near the Z peak,

$$a = \frac{\int a_2 \, d\Omega}{\int a_1 \, d\Omega} = 8 \, \beta \, \frac{g_v g_A}{(3 + \beta^2)\,(g_v^{\,2} + g_A^{\,2}) + \frac{3}{\gamma^2}\,(g_v^{\,2} - g_A^{\,2})} \tag{5a}$$

$$b = \frac{\int a_3 \, d\Omega}{\int a_1 \, d\Omega} = \frac{(1 + 3\beta^2)\,(g_v^{\,2} + g_A^{\,2}) + \frac{1}{\gamma^2}\,(g_v^{\,2} - g_A^{\,2})}{(3 + \beta^2)\,(g_v^{\,2} + g_A^{\,2}) + \frac{3}{\gamma^2}\,(g_v^{\,2} - g_A^{\,2})} \, . \tag{5b}$$

They reduce in the limits $\beta \to 0$ and $\beta \to 1$, to

$$a = \frac{8}{3}\,\frac{g_A}{g_v}\,\beta \, , \quad b = \frac{1}{3} \qquad (\beta \to 0) \tag{6a}$$

$$a = \frac{2\, g_v\, g_A}{g_v^{\,2} + g_A^{\,2}} \, , \quad b = 1 \qquad (\beta = 1) \, . \tag{6b}$$

Single particle spectra can be recovered by integrating eq. (4) over either X_1 or X_2. For example, upon integration over X_2, we get

$$\frac{1}{\Gamma_i}\,\frac{d\Gamma_i}{dX_1} = F_i\,(X_1) + a\, G_i\,(X_1) \, , \tag{7}$$

where we have used

$$\int F_i\,(X)\, dX = 1 \tag{8a}$$

$$\int G_i\,(X)\, dX = 0 \, , \tag{8b}$$

the range of integration depending on whether it is for ℓ or π (eqs. (2.3), (3.3)).

a is nothing other than $\langle P_L \rangle$, and eq. (7) is identical to eqs. (2.7) and (3.2).

One quantity containing information on the spin correlation is the following

$$\Delta = \frac{1}{\sigma_c} \frac{d\sigma_c}{dX_1\, dX_2} - \left[\frac{1}{\Gamma_i} \frac{d\Gamma_i}{dX_1}\right] \left[\frac{1}{\Gamma_j} \frac{d\Gamma_j}{dX_2}\right] \tag{9a}$$

$$= (b - a^2)\, G_i\,(X_1)\, G_j\,(X_2) \tag{9b}$$

$$= 4\, \frac{(-\beta^4 + 2\beta^2 + 3)\, g_v^{\,4} + 4\beta^4\, g_A^{\,4} - 8\beta^2\, g_v^{\,2}\, g_A^{\,2}}{[(3 + \beta^2)\,(g_v^{\,2} + g_A^{\,2}) + \frac{3}{\gamma^2}\,(g_v^{\,2} - g_A^{\,2})]^2}\, G_i(X_1)\, G_j(X_2) \tag{9c}$$

Experimentally Δ represents the difference between the normalized spectrum for coincident decays and the product of two independent single decay spectra.

For $\beta = 1$, Δ reduces to:

$$\Delta = [1 - \langle P_L \rangle^2]\, G_i\,(X_1)\, G_j\,(X_2)\ , \tag{10}$$

and is still parametrized by the same quantity as in the single particle spectrum case. Only for appreciably smaller values of β , b (eq. 5(b)) is different from unity and provides non-trivial information.

Our approach has been that we first treated the two steps in the process (eq. (1)) sparately, and reduced the expressions in

terms of the 3-spins in heavy lepton rest frames, which were then summed over. We note in closing that other authors [8] have used, in the simple case of $\beta = 1$, the covariant formalism in which L^+L^- are treated as intermediate states. The heavy lepton propagators used in computing the process (1) are then put on mass shell via the substitution $\frac{1}{(p^2 - M_L^2)^2 + M_L^2 \Gamma^2} \to \frac{\pi}{M_L \Gamma} \delta (p^2 - M_L^2)$.

FIGURE CAPTIONS

Fig. 1 Tree level diagrams used in computing the spin-dependent cross-section for $e^+e^- \to L^+L^-$.

Fig. 2 The coordinate system used in deriving formulas in this chapter.

Fig. 3 Plots of $F_\ell(X)$ and $G_\ell(X)$ for various values of β .

Fig. 4 Plots of $\frac{1}{\Gamma_\pi}\frac{d\Gamma_\pi}{dX}$ for various values of β with $\sin^2\theta_W = .2$.

REFERENCES

[1] S. Glashow, Nucl. Phys. 22, 579 (1961); S. Weinberg, Phys. Rev. Lett. 19, 1264 (1967); A. Salam, in 8th Nobel Symp. ed. N. Svartholm, p. 367 (1968).

[2] See, for example, MARK J Collab., MIT Technical Report #124 (1982).

[3] Y. S. Tsai, Phys. Rev. D 4, 2821 (1971).

[4] R. Budny, Phys. Lett. 55 B, 227 (1975).

[5] G. Goggi, ECFA/LEP/2; ECFA/LEP/4 (1978); G. Goggi, Nuo. Cim. Lett. 24, 49 (1979).

[6] J. E. Augustin, ECFA/LEP/29 (1978).

[7] S. V. Golovkin et al., Nucl. Inst. Meth. 138, 235 (1976).

[8] F. Bletzacker and H. T. Nieh, Phys. Rev. D 14, 1251 (1976).

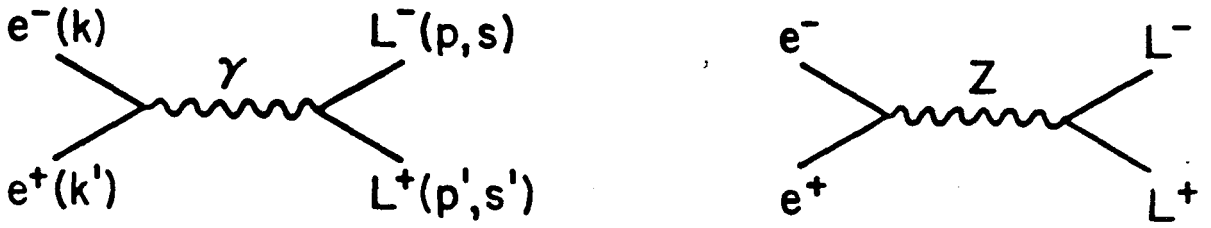

FIG. 1

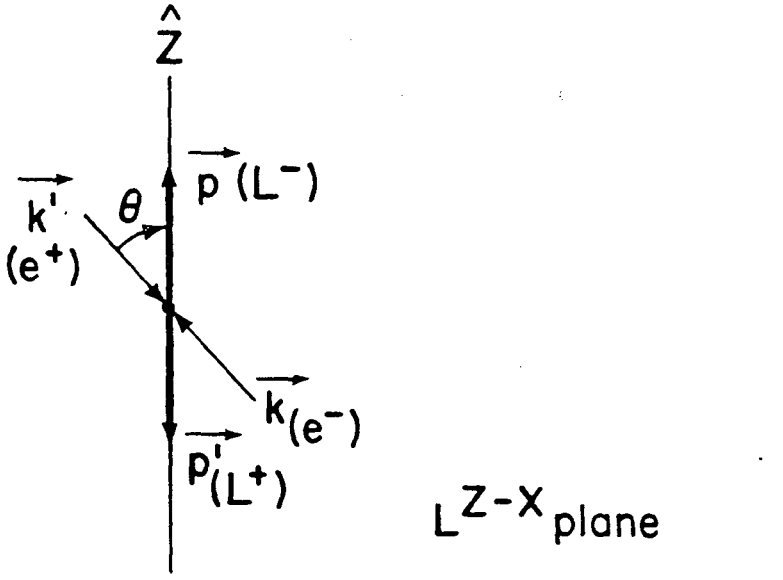

XBL-827-7231

FIG. 2

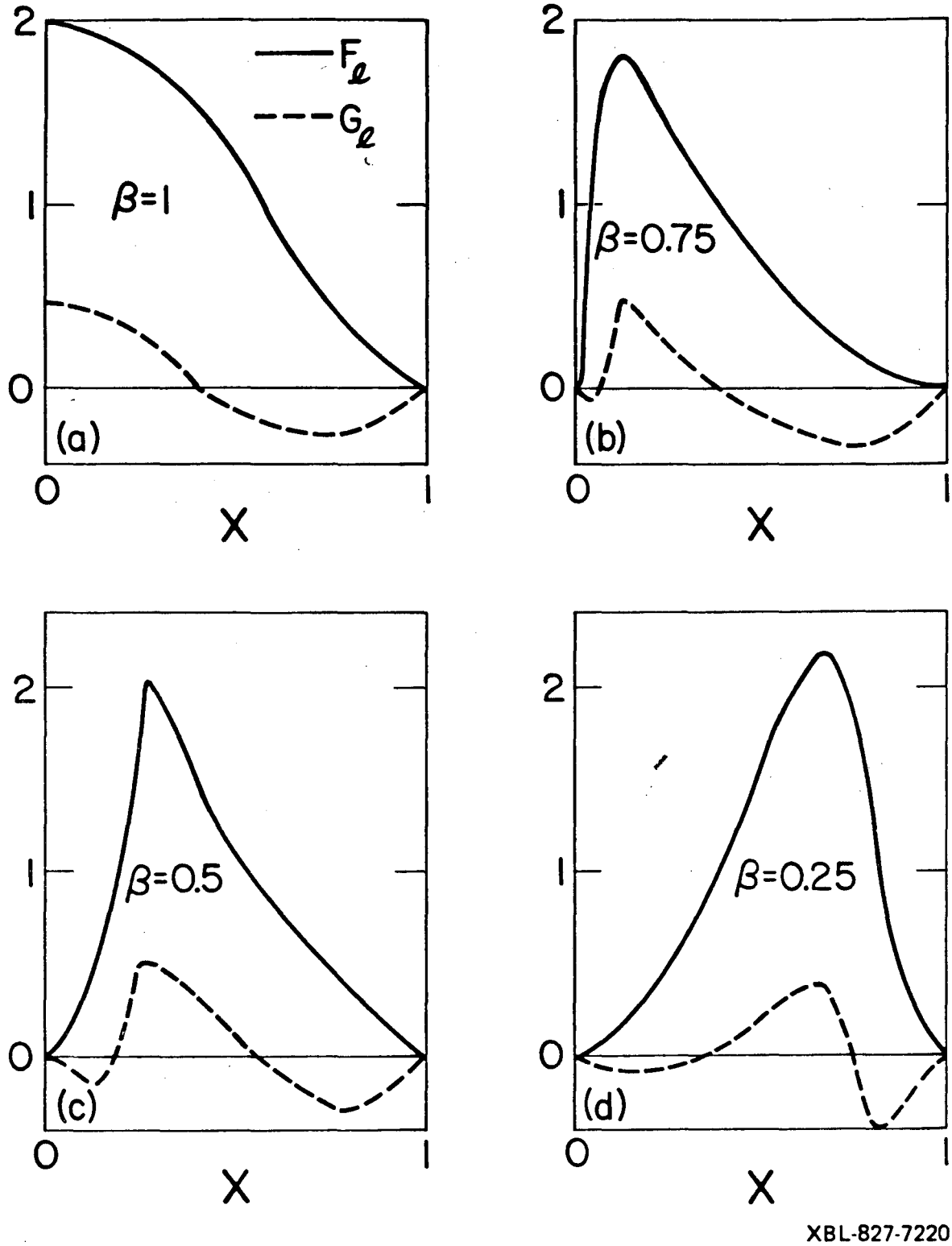
2
1
0
F_ℓ
G_ℓ
β=1
(a)
0
1
X
2
1
0
β=0.75
(b)
0
1
X
2
1
0
β=0.5
(c)
0
1
X
2
1
0
β=0.25
(d)
0
1
X
XBL-827-7220

FIG. 3

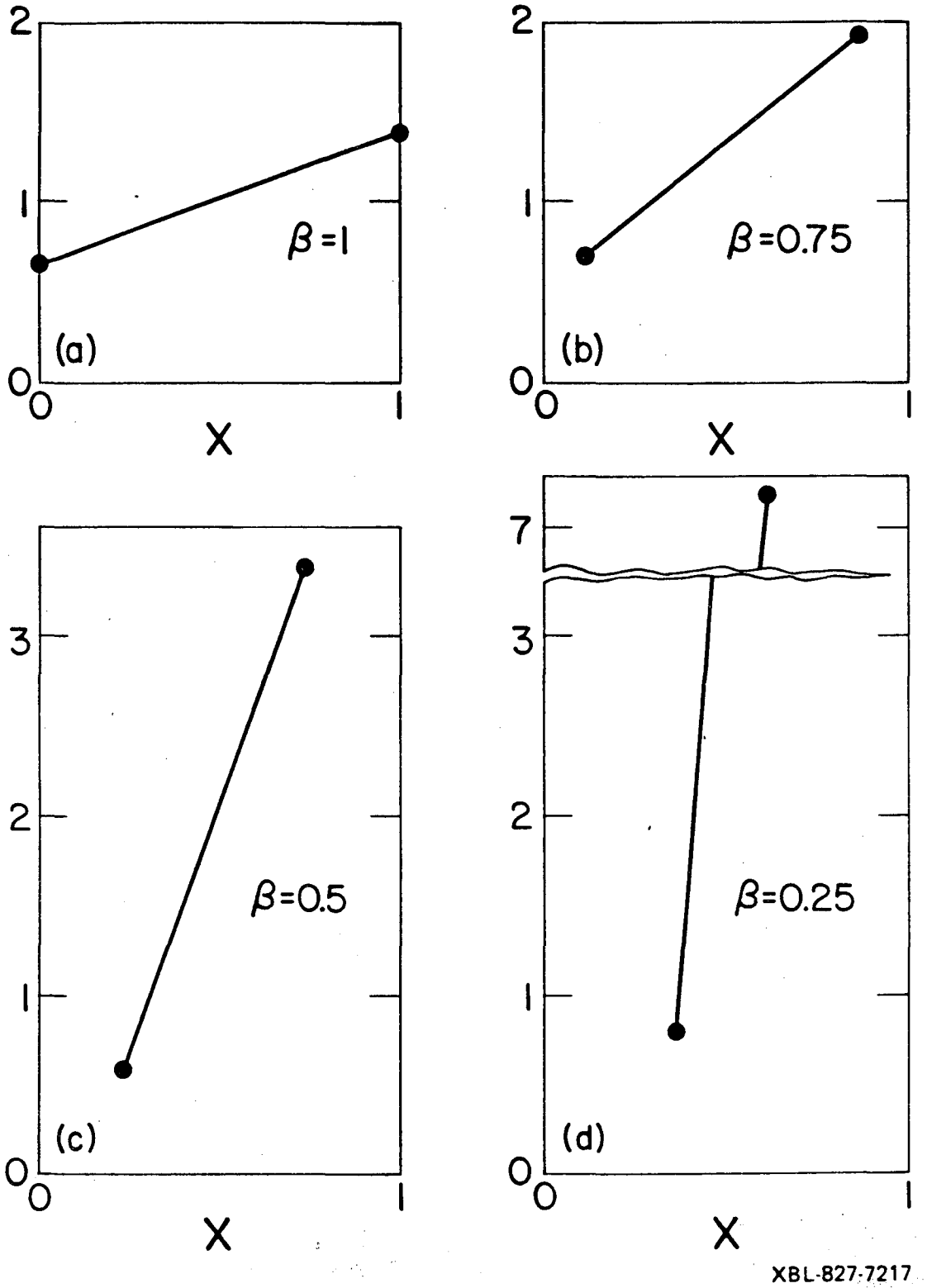

XBL-827-7217

FIG. 4

This report was done with support from the Department of Energy. Any conclusions or opinions expressed in this report represent solely those of the author(s) and not necessarily those of The Regents of the University of California, the Lawrence Berkeley Laboratory or the Department of Energy.

Reference to a company or product name does not imply approval or recommendation of the product by the University of California or the U.S. Department of Energy to the exclusion of others that may be suitable.

TECHNICAL INFORMATION DEPARTMENT
LAWRENCE BERKELEY LABORATORY
UNIVERSITY OF CALIFORNIA
BERKELEY, CALIFORNIA 94720